

AD-A134 706

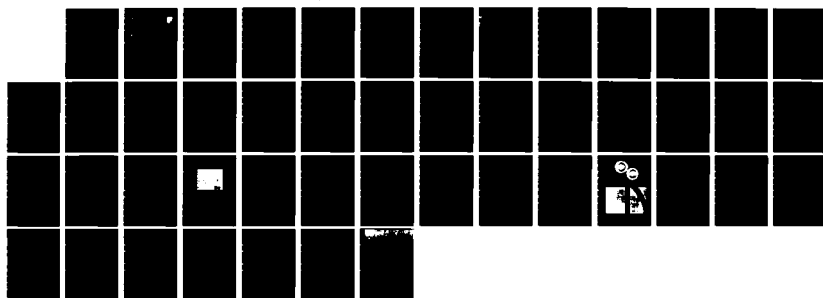
LITHOGRAPHY RADIATION EFFECTS STUDY(U) SPIRE CORP
BEDFORD MA B MURRAY SEP 83 IR-10076 RADC-TR-83-229
F19628-80-C-0196

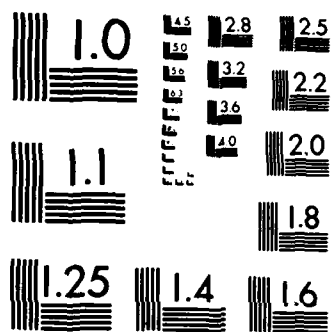
1/1

UNCLASSIFIED

F/G 14/5

NL





MICROCOPY RESOLUTION TEST CHART
NATIONAL BUREAU OF STANDARDS-1963-A

AD-A134706

RADC-TR-83-229
Interim Report
September 1983

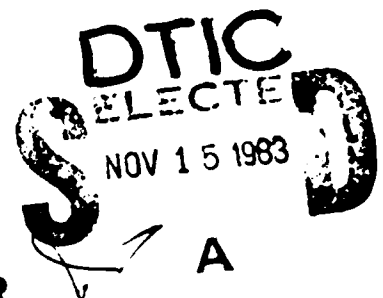


LITHOGRAPHY RADIATION EFFECTS STUDY

Spire Corporation

Brian Murray

APPROVED FOR PUBLIC RELEASE; DISTRIBUTION UNLIMITED



ROME AIR DEVELOPMENT CENTER
Air Force Systems Command
Griffiss Air Force Base, NY 13441

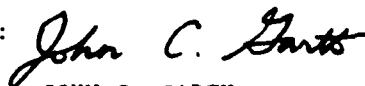
DTIC FILE COPY

83 11 15 053

This report has been reviewed by the RADC Public Affairs Office (PA) and is releasable to the National Technical Information Service (NTIS). At NTIS it will be releasable to the general public, including foreign nations.

RADC-TR-83-229 has been reviewed and is approved for publication.

APPROVED:



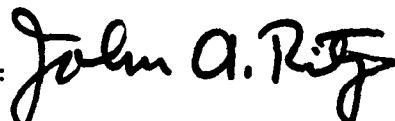
JOHN C. GARTH
Project Engineer

APPROVED:



HAROLD ROTH, Director
Solid State Sciences Division

FOR THE COMMANDER:



JOHN A. RITZ
Acting Chief, Plans Office

If your address has changed or if you wish to be removed from the RADC mailing list, or if the addressee is no longer employed by your organization, please notify RADC (ESRE), Hanscom AFB MA 01731. This will assist us in maintaining a current mailing list.

Do not return copies of this report unless contractual obligations or notices on a specific document requires that it be returned.

UNCLASSIFIED

SECURITY CLASSIFICATION OF THIS PAGE (When Data Entered)

REPORT DOCUMENTATION PAGE		READ INSTRUCTIONS BEFORE COMPLETING FORM
1. REPORT NUMBER RADC-TR-83-229	2. GOVT ACCESSION NO. AD-A134	3. RECIPIENT'S CATALOG NUMBER 706
4. TITLE (and Subtitle) LITHOGRAPHY RADIATION EFFECTS STUDY		5. TYPE OF REPORT & PERIOD COVERED Interim Report 20 Nov 80 - 20 May 82
		6. PERFORMING ORG. REPORT NUMBER IR-10076
7. AUTHOR(s) Brian Murray		8. CONTRACT OR GRANT NUMBER(s) F19628-80-C-0196
9. PERFORMING ORGANIZATION NAME AND ADDRESS Spire Corporation Patriots Park Bedford MA 01730		10. PROGRAM ELEMENT, PROJECT, TASK AREA & WORK UNIT NUMBERS 61102F 2306J331
11. CONTROLLING OFFICE NAME AND ADDRESS Rome Air Development Center (ESRE) Hanscom AFB MA 01731		12. REPORT DATE September 1983
		13. NUMBER OF PAGES 50
14. MONITORING AGENCY NAME & ADDRESS (if different from Controlling Office) Same		15. SECURITY CLASS. (of this report) UNCLASSIFIED
		15a. DECLASSIFICATION/DOWNGRADING SCHEDULE N/A
16. DISTRIBUTION STATEMENT (of this Report) Approved for public release; distribution unlimited.		
17. DISTRIBUTION STATEMENT (of the abstract entered in Block 20, if different from Report) Same		
18. SUPPLEMENTARY NOTES RADC Project Engineer: John C. Garth (ESRE)		
19. KEY WORDS (Continue on reverse side if necessary and identify by block number) X-ray Lithography Dose Profile Measurement Technique PBS Resist X-Ray Photoelectrons		
20. ABSTRACT (Continue on reverse side if necessary and identify by block number) An experimental x-ray lithography facility for irradiation thin films of a photoresist next to a gold mask is described. The x-ray irradiance and PMMA irradiation times are estimated for several target elements with characteristic x-ray lines in the 1-3 KeV energy range. Gold masks deposited with films of carbon 100, 220, 520 and 710 Angstroms thick were placed next to films of PBS resist and irradiated with x-rays from Al, Ag, and Ti targets bombarded by 10 KeV electrons. The exposed PBS was etched		

DD FORM 1 JAN 73 1473

EDITION OF 1 NOV 55 IS OBSOLETE

UNCLASSIFIED

SECURITY CLASSIFICATION OF THIS PAGE (When Data Entered)

SECURITY CLASSIFICATION OF THIS PAGE(When Data Entered)

Accession of
1955-1956
1957-1958
1959-1960
1961-1962
1963-1964
1965-1966
1967-1968
1969-1970
1971-1972
1973-1974
1975-1976
1977-1978
1979-1980
1981-1982
1983-1984
1985-1986
1987-1988
1989-1990
1991-1992
1993-1994
1995-1996
1997-1998
1999-2000
2001-2002
2003-2004
2005-2006
2007-2008
2009-2010
2011-2012
2013-2014
2015-2016
2017-2018
2019-2020
2021-2022
2023-2024
2025-2026
2027-2028
2029-2030
2031-2032
2033-2034
2035-2036
2037-2038
2039-2040
2041-2042
2043-2044
2045-2046
2047-2048
2049-2050
2051-2052
2053-2054
2055-2056
2057-2058
2059-2060
2061-2062
2063-2064
2065-2066
2067-2068
2069-2070
2071-2072
2073-2074
2075-2076
2077-2078
2079-2080
2081-2082
2083-2084
2085-2086
2087-2088
2089-2090
2091-2092
2093-2094
2095-2096
2097-2098
2099-2100
2101-2102
2103-2104
2105-2106
2107-2108
2109-2110
2111-2112
2113-2114
2115-2116
2117-2118
2119-2120
2121-2122
2123-2124
2125-2126
2127-2128
2129-2130
2131-2132
2133-2134
2135-2136
2137-2138
2139-2140
2141-2142
2143-2144
2145-2146
2147-2148
2149-2150
2151-2152
2153-2154
2155-2156
2157-2158
2159-2160
2161-2162
2163-2164
2165-2166
2167-2168
2169-2170
2171-2172
2173-2174
2175-2176
2177-2178
2179-2180
2181-2182
2183-2184
2185-2186
2187-2188
2189-2190
2191-2192
2193-2194
2195-2196
2197-2198
2199-2200
2201-2202
2203-2204
2205-2206
2207-2208
2209-2210
2211-2212
2213-2214
2215-2216
2217-2218
2219-2220
2221-2222
2223-2224
2225-2226
2227-2228
2229-2230
2231-2232
2233-2234
2235-2236
2237-2238
2239-2240
2241-2242
2243-2244
2245-2246
2247-2248
2249-2250
2251-2252
2253-2254
2255-2256
2257-2258
2259-2260
2261-2262
2263-2264
2265-2266
2267-2268
2269-2270
2271-2272
2273-2274
2275-2276
2277-2278
2279-2280
2281-2282
2283-2284
2285-2286
2287-2288
2289-2290
2291-2292
2293-2294
2295-2296
2297-2298
2299-2300
2301-2302
2303-2304
2305-2306
2307-2308
2309-2310
2311-2312
2313-2314
2315-2316
2317-2318
2319-2320
2321-2322
2323-2324
2325-2326
2327-2328
2329-2330
2331-2332
2333-2334
2335-2336
2337-2338
2339-2340
2341-2342
2343-2344
2345-2346
2347-2348
2349-2350
2351-2352
2353-2354
2355-2356
2357-2358
2359-2360
2361-2362
2363-2364
2365-2366
2367-2368
2369-2370
2371-2372
2373-2374
2375-2376
2377-2378
2379-2380
2381-2382
2383-2384
2385-2386
2387-2388
2389-2390
2391-2392
2393-2394
2395-2396
2397-2398
2399-2400
2401-2402
2403-2404
2405-2406
2407-2408
2409-2410
2411-2412
2413-2414
2415-2416
2417-2418
2419-2420
2421-2422
2423-2424
2425-2426
2427-2428
2429-2430
2431-2432
2433-2434
2435-2436
2437-2438
2439-2440
2441-2442
2443-2444
2445-2446
2447-2448
2449-2450
2451-2452
2453-2454
2455-2456
2457-2458
2459-2460
2461-2462
2463-2464
2465-2466
2467-2468
2469-2470
2471-2472
2473-2474
2475-2476
2477-2478
2479-2480
2481-2482
2483-2484
2485-2486
2487-2488
2489-2490
2491-2492
2493-2494
2495-2496
2497-2498
2499-2500
2501-2502
2503-2504
2505-2506
2507-2508
2509-2510
2511-2512
2513-2514
2515-2516
2517-2518
2519-2520
2521-2522
2523-2524
2525-2526
2527-2528
2529-2530
2531-2532
2533-2534
2535-2536
2537-2538
2539-2540
2541-2542
2543-2544
2545-2546
2547-2548
2549-2550
2551-2552
2553-2554
2555-2556
2557-2558
2559-2560
2561-2562
2563-2564
2565-2566
2567-2568
2569-2570
2571-2572
2573-2574
2575-2576
2577-2578
2579-2580
2581-2582
2583-2584
2585-2586
2587-2588
2589-2590
2591-2592
2593-2594
2595-2596
2597-2598
2599-2600
2601-2602
2603-2604
2605-2606
2607-2608
2609-2610
2611-2612
2613-2614
2615-2616
2617-2618
2619-2620
2621-2622
2623-2624
2625-2626
2627-2628
2629-2630
2631-2632
2633-2634
2635-2636
2637-2638
2639-2640
2641-2642
2643-2644
2645-2646
2647-2648
2649-2650
2651-2652
2653-2654
2655-2656
2657-2658
2659-2660
2661-2662
2663-2664
2665-2666
2667-2668
2669-2670
2671-2672
2673-2674
2675-2676
2677-2678
2679-2680
2681-2682
2683-2684
2685-2686
2687-2688
2689-2690
2691-2692
2693-2694
2695-2696
2697-269

SECURITY CLASSIFICATION OF THIS PAGE (When Data Entered)



TABLE OF CONTENTS

<u>Section</u>	<u>Page</u>
1.0 INTRODUCTION	1
2.0 X-RAY LITHOGRAPHY EXPERIMENTAL FACILITY	2
2.1 X-Ray Source Vacuum Chamber	2
2.2 Electron Gun	2
2.2.1 General Description	2
2.2.2 Electron Gun Configuration Within the Vacuum Chamber	4
2.2.3 Focus Coil Adaptation	6
2.3 X-Ray Target Anode Assembly	6
2.4 Residual Gas Analyzer (RGA) and Viewing Window	8
2.5 Faraday Cup Electron Beam Monitor and Electron Trap	8
3.0 PRODUCTION OF X-RAYS	12
3.1 Estimated X-ray Irradiance and PMMA Exposure Times	12
3.2 Experimental Check of Calculation	14
3.3 Dosimetry	14
4.0 INITIAL MEASUREMENTS USING A RESIST MATERIAL	16
4.1 Electron Beam Evaporator	16
4.2 Photoresist Materials as Dosimeters	16
4.3 X-Ray Irradiation of PBS	19
4.4 Poly (Butene-1 Sulfone) (PBS) Resist as a Detector	21
4.5 Experiments with an X-ray Mask	21
5.0 DOSE PROFILE MEASUREMENTS USING PBS RESIST	23
5.1 Rationale for Experimental Approach	23
5.2 High Z/Low Z X-ray Masks	25
5.2.2 Metal Evaporation	25
5.2.3 Carbon Deposition on X-ray Masks	29
5.2.4 Gold/Carbon Mask	29
5.2.5 Silver/Carbon Mask	30
5.2.6 Spinning of the PBS Resist on Silicon Wafers	32
5.2.7 X-ray Irradiations	32
5.2.8 Resist Development	33
6.0 MEASUREMENTS AND RESULTS OF DOSE PROFILES	33
6.1 Ellipsometer Measurements	33
6.2 Measurement Results	36
6.3 Comment on Dose Profile Data	36
REFERENCES	39

LIST OF ILLUSTRATIONS

<u>Figures</u>		<u>Page</u>
1	Top View Illustration of Vacuum Chamber Configuration	3
2	Schematic Sketch of Electron Beam Gun Mount Within Vacuum Chamber	5
3	Schematic Sketch of X-ray Target Anode Assembly	7
4	Full Size Assembly Drawing of Faraday Cup and Electron Trap	9
5	Schematic View of Electron Trap	10
6	X-Ray Absorption Coefficient for Poly(Methyl Methacrylate), $H_8C_5O_2$ PMMA	15
7	E-Beam Evaporator Apparatus for X-ray Irradiations	17
8	Characteristic Exposure Curve for PBS Using AgL Radiation	18
9	X-ray Absorption Coefficient and Transmission for Poly(Butene-1-Sulfone) Resist	20
10	Dektak Thickness Measurements of PBS Spun Coatings on Si Wafers	22
11	Developed X-ray mask Pattern Using PBS	24
12	Experimental Configuration for Measuring Dose Profiles Near Au/C Interface	26
13	Dektak Measurements on Glass of Carbon and Au Layer Thicknesses	27
14	Dektak Measurements of the Ag Evaporation onto Mylar Pellicle	28
15	Photograph of the Au/C and Ag/C X-ray Masks	31
16	Nomarski (DIC) Photomicrograph of Selected Regimes of the Experimental X-ray Masks: A-Au/C Mask and B-Ag/C Mask	31
17	ψ and Δ vs. Refractive Index and Thickness of Transparent Film on Silicon Substrates	35
18	Dose Profiles in PBS Resist Using Au/C Mask	38

1.0 INTRODUCTION

The X-Ray Lithography Radiation Effects Contract (No. F19628-80-C-0196) is a 30-month program which has the following major objectives:

- a. The development of methods for submicron depth dose measurements in low Z materials in the vicinity of interfaces with high Z materials. The measurements will be restricted to one-dimensional geometries, and will measure the dose contributions of 1-10 keV characteristic x-rays, continuum x-rays, and electrons produced in the high Z material.
- b. One method to be developed will physically measure energy deposited in materials by monitoring transmitted radiations with a solid state detector. The detector will also provide additional information on the transmitted photoelectron spectrum as well as the x-ray spectrum.
- c. The second method to be developed will be dose profile measurements in low Z materials using well characterized photoresists as detectors.
- d. The comparison of experimental data with calculational results of available codes and theoretical models to check the accuracy of these calculational methods.
- e. The development of a list of guidelines based on the results of this program to help optimize further work in x-ray lithography.

Commercial x-ray sources, with the flexibility for performing the measurements necessary for this program, are not available. As a result, a major part of the initial effort is, therefore, the design and assembly of a highly reliable, variable energy x-ray source. This source is not designed to have high brightness, but it will be intensity and voltage stabilized.

The techniques by which thin films (filters, photoresist, oxides, etc.) are constructed and the accuracy to which their dimensions are known are critical in obtaining reliable data. In addition, techniques will need to be developed to utilize photoresist materials as sensitive dose monitors. A second major element, then, in

the initial efforts of this program will be to fully develop and utilize these techniques for this program. Spire Corporation will employ its internal semiconductor processing laboratory to fabricate precision films using photoresist spinning, evaporation and sputtering methods.

2.0 X-RAY LITHOGRAPHY EXPERIMENTAL FACILITY

2.1 X-Ray Source Vacuum Chamber

After a thorough review, the vacuum chamber illustrated in Figure 1 was chosen to house the x-ray source and experimental components. The outside diameter of the main chamber is 6 inches, with the largest conflat flanges being 8-inches in diameter. Six vacuum ports have rotatable conflat flanges. This chamber design allows for the flexibility needed for the experimental studies. The two ports along the vertical direction (normal to page) connect to the vacuum pump (below) and other experiments (above). The four horizontal ports in the plane of the page will house the x-ray target anode, the electron gun, the residual gas analyzer (RGA), and the Faraday cup electron beam monitor.

Oil-free vacuum pumping is accomplished with a 30 l s^{-1} ion pump with a sorption pump for initial rough pumping. The 1-1/2-inch pumpout port in Figure 1 is used to rough pump the chamber. A bake-out mantle is needed to bake out the chamber to at least 200°C so that ultra high vacuum (UHV) pressures of residual gases can be realized. The RGA will be especially useful in determining the quality of the vacuum environment of the chamber, and can be used to detect the presence of leaks and to monitor the effectiveness of various bake-out procedures.

The vacuum system was tested to pump down the bare vacuum chamber closed off with conflat flanges. With minimum chamber bakeout (using heating tapes), the vacuum pressure obtained was 2×10^{-7} torr.

2.2 Electron Gun

2.2.1 General Description

After an extensive search, a suitable electron gun was purchased from Nuclide Corporation of Acton. It is designed for 30 kV, 300 mA operation, but the upper limits of the HV power supply is 15 kV and 50 mA. The current regulation is 1 percent or better, while the voltage regulation is better than 5 percent.

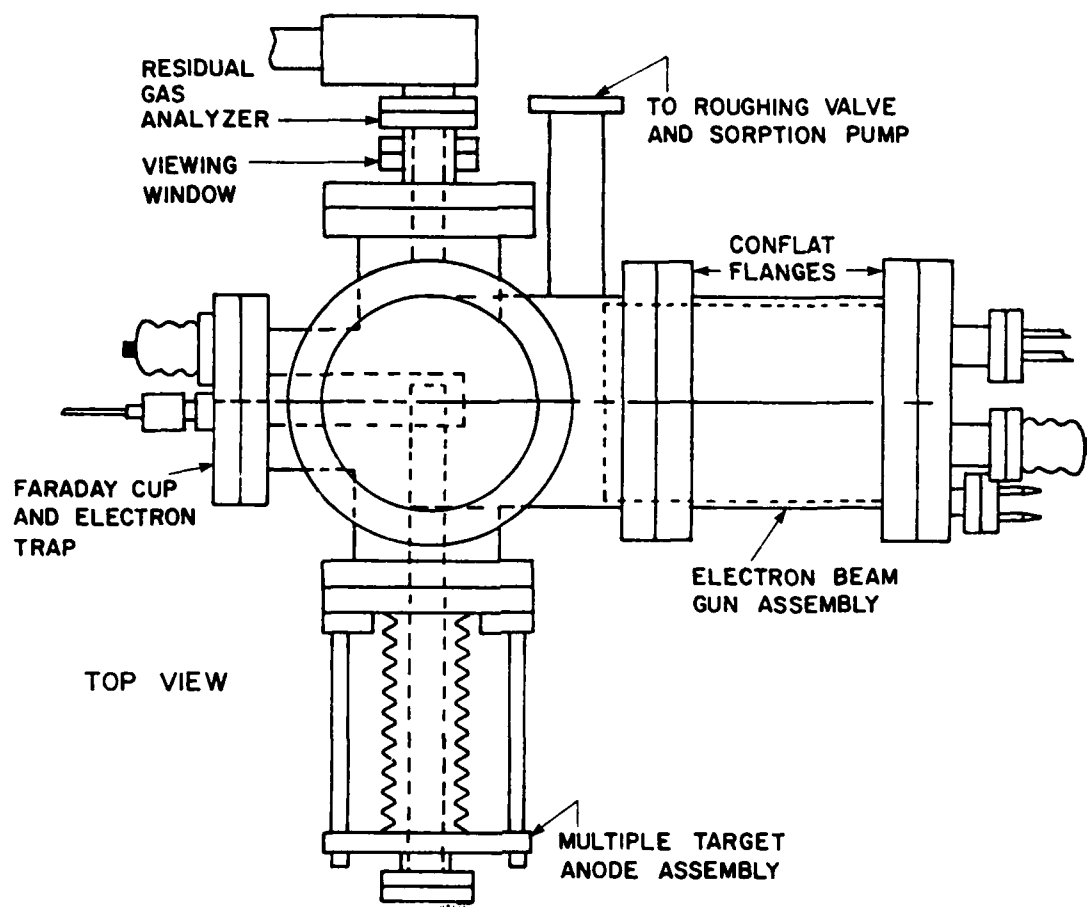


FIGURE 1. TOP VIEW ILLUSTRATION OF VACUUM CHAMBER CONFIGURATION.
(The conflat flanges contain Cu-metal-gaskets which provide the UHV seals.)

The gun comes as a system with power supplies and controls which can operate in a stable fashion in the microamp range as well as at 50 mA. This is due to a manually adjusted anode-cathode gap in the gun assembly. The lowest accelerating voltage at which it can operate in a stable manner and with some current is not yet fully known. This gun model has been shown by other users to yield up to 84 mA when operated at 5 kV. The chances of operating it at 3 kV with a stable current are very good. Since the cathode can be adjusted to change the perveance ($I(\text{amps})/V^{3/2}$), a current of 20 mA and an operating voltage of 2.2 kV yields a perveance of 2×10^{-7} . As long as the perveance is below 10^{-6} , stable operation should be obtainable.

The electron beam is focused with a magnetic coil which allows the distance between the coil and the anode target to be very large. This gun model has been operated at an 18-inch working distance with a 4-mm spot size. The filament material (Ta ribbon) has a vapor pressure of 6×10^{-7} torr at its surface when operated at 2200°C. Neutral Ta atoms can be boiled off and land on any cold, nearby surface. Having the capability of a long working distance minimizes the risk of contaminating an x-ray anode target surface with Ta from the cathode. Nevertheless, direct site between the filament and anode target does imply eventual contamination of the target with Ta.

2.2.2 Electron Gun Configuration Within the Vacuum Chamber

Although the electron gun is a purchased component, a significant amount of engineering effort was required to insure that this component will perform with the flexibility required for this program. In order to steer the electron beam to the x-ray target anode, the gun must first be mounted properly inside the vacuum chamber so that adjustments can be made. Figure 2 is a schematic sketch illustrating the mounting of the gun and its focus coil within the 6-inch tubulation off the main vacuum chamber. The electron gun body is fastened to two OFHC copper plates which, in turn, are attached to an adjustable copper plate by two (or three) 1/2-inch copper rods. This kind of mechanical adjustment will be necessary, also, for the x-ray target anode assembly and the electron trap. By making proper adjustments to this plate, the direction of the electron beam will be aimed toward the x-ray target anode. This plate, in turn, is attached to the 8-inch (O.D.) conflat flange which has the feedthroughs for high voltage, focus coil current and cooling water. The cooled copper vacuum shroud is necessary to shield the source housing from the heat generated by the electron gun, during long operating periods.

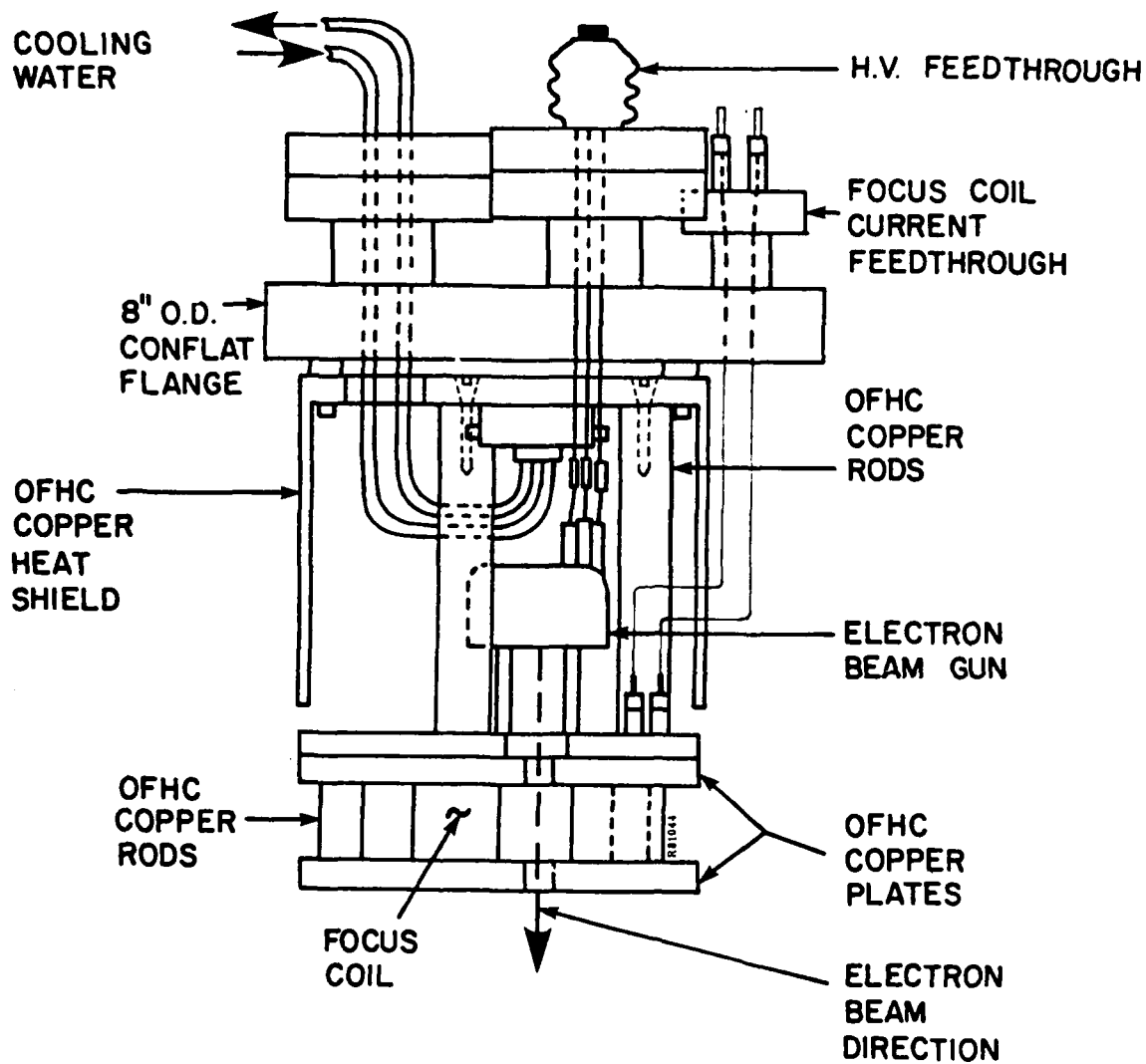


FIGURE 2. SCHEMATIC SKETCH OF ELECTRON BEAM GUN MOUNT WITHIN VACUUM CHAMBER (not to scale)

2.2.3 Focus Coil Adaptation

The focus coil, as supplied by Nuclide Corporation, was adapted for use in an UHV environment. The least costly way to adapt this coil for a UHV environment was to encapsulate it in a welded, vacuum-tight steel canister. Vacuum feedthroughs were used to bring the coil leads out of the canister. Since up to 20 watts of electrical power can be fed to the focus coil during operation, cooling of the coil is necessary. This is accomplished by placing the canister between copper plates which are water cooled through the 1/2-inch copper support rods. There are no demountable waterline connections within the electron gun mounting configuration. The coil itself is potted within the canister under vacuum to insure a long service life and to promote heat conduction from the coil to the water-cooled copper plates.

2.3 X-Ray Target Anode Assembly

Since the program calls for a variety of x-ray energies, a means of changing the energies of the x-rays produced had to be devised. To provide the means to change the energy of the characteristic x-ray produced in this facility, a moveable anode assembly was designed as illustrated in Figure 3. The x-ray anode is a water-cooled, multiple target, designed for remote positioning in the electron beam. The main anode body will have a cross section approximately 1-inch square and 4-inches long. It will be bevelled at the end which faces the incident electron beam. Selected x-ray target materials, such as aluminum, silver, titanium and chromium will be deposited on the substrate at well specified locations.

Each of these target materials can be brought into alignment with the electron beam by moving the anode linearly in or out of the chamber as permitted by the linear motion feedthrough arrangement. A long welded metal type bellows provides about 5 inches of linear movement. The motion feedthrough is designed to provide small amounts of lateral and tilting adjustment similar to the kind of adjustments for the electron beam gun.

When the bevelled end of the anode body is brought into alignment with the electron beam, the spot formed by the beam can be viewed through a 1-1/2-inch diameter viewing window placed in the vacuum port opposite the anode port. Beam focussing can be accomplished with the anode in this position. The anode may be also fully retracted from the beam so that the electron beam strikes a Faraday cup collector fixed in the beam line behind the anode.

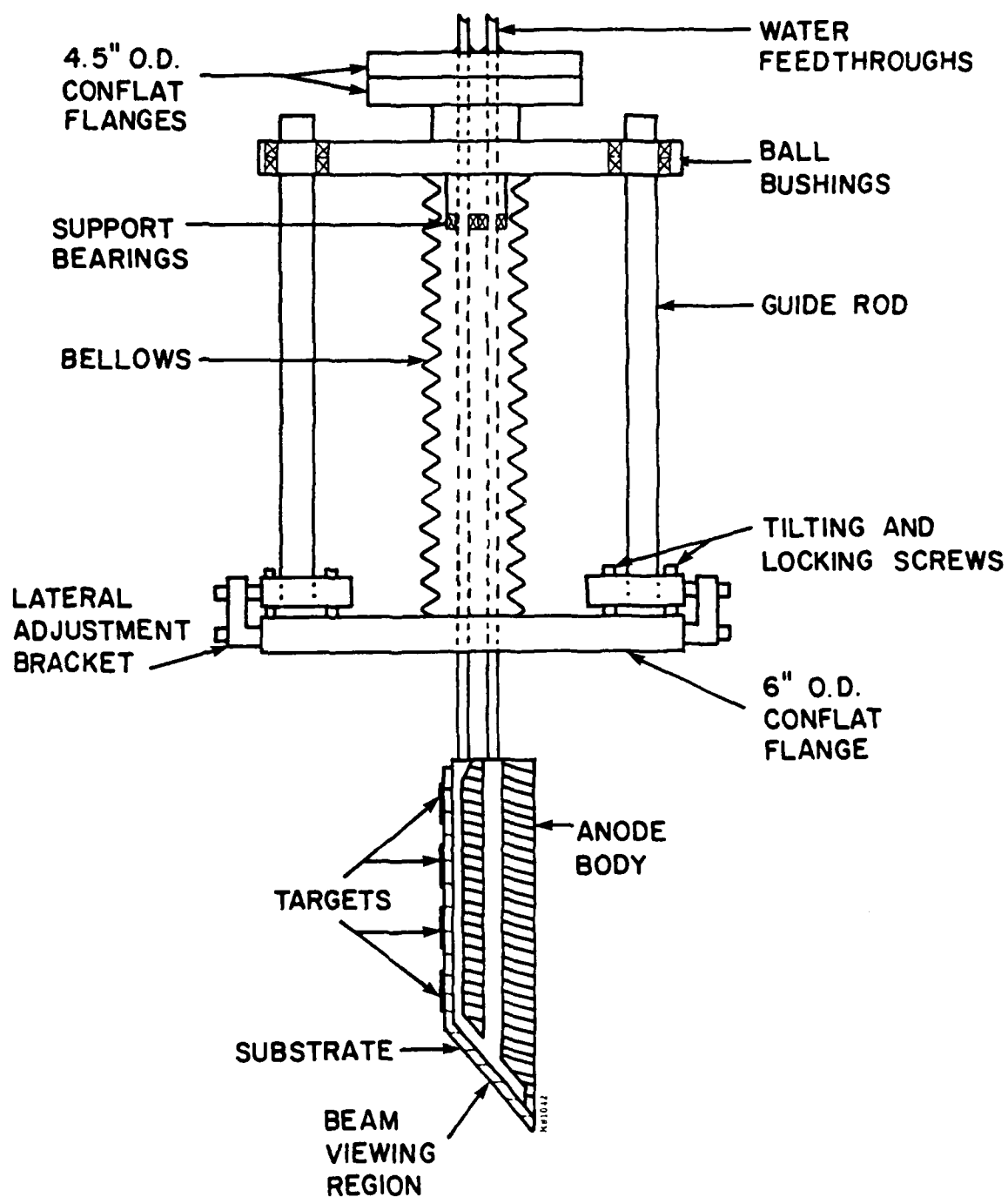


FIGURE 3. SCHEMATIC SKETCH OF X-RAY TARGET ANODE ASSEMBLY
 (To change an x-ray target element, the anode assembly manually moved externally to align a new target element in the electron beam.)

Water cooling of the anode target is necessary to allow as much electron beam power on target as possible before melting occurs. The maximum power is 750 watts (15 keV, 50 mA). Because of the high water flow rate anticipated, a closed circulating distilled water system will probably be needed to insure trouble-free water cooling of the anode body.

2.4 Residual Gas Analyzer (RGA) and Viewing Window

An important component of the vacuum system will be an RGA mounted to the vacuum port opposite the x-ray anode assembly port (see Figure 1). The RGA will be a commercial quadropole mass spectrometer and will extend into the 4-inch housing tabulation a small distance. Mounted alongside the RGA on the 6-inch (O.D.) conflat flange will be a 1-1/2-inch diameter viewing window. This window is mounted within a 2-3/4-inch conflat flange and small tubulation to provide a direct view of the anode assembly. The electron beam spot should be visible when the anode body is placed so that the beam strikes the bevelled end of the anode body.

2.5 Faraday Cup Electron Beam Monitor and Electron Trap

The engineering assembly drawing for the Faraday cup monitor and electron trap is shown in Figure 4. The monitor has a deep cup (2 3/4 inches) and a suppressor electrode to capture all the incident electrons. This design should ensure a true measurement of the electron beam current. The enclosure is grounded, and the current measuring lead is shielded electrostatically to reduce noise and pickup from the nearby high voltage leads. The Faraday cup, fixed to a solid boron nitride base, also forms the support for the electron trap.

The electron trap is a parallelopiped with four copper sides and two graphite collimators. A high voltage lead (with the same potential as the accelerating voltage) passes through one of the copper walls to form an electrostatic field transverse to the x-ray beam. The choice of graphite for the collimator material has been made initially on the basis of low cost.

Figure 5 is a schematic illustration of the electron trap. When the anode body is pulled out of the way, the electron beam is incident upon the Faraday cup. When the anode is in a selected position, x-rays are generated in, and electrons are scattered from

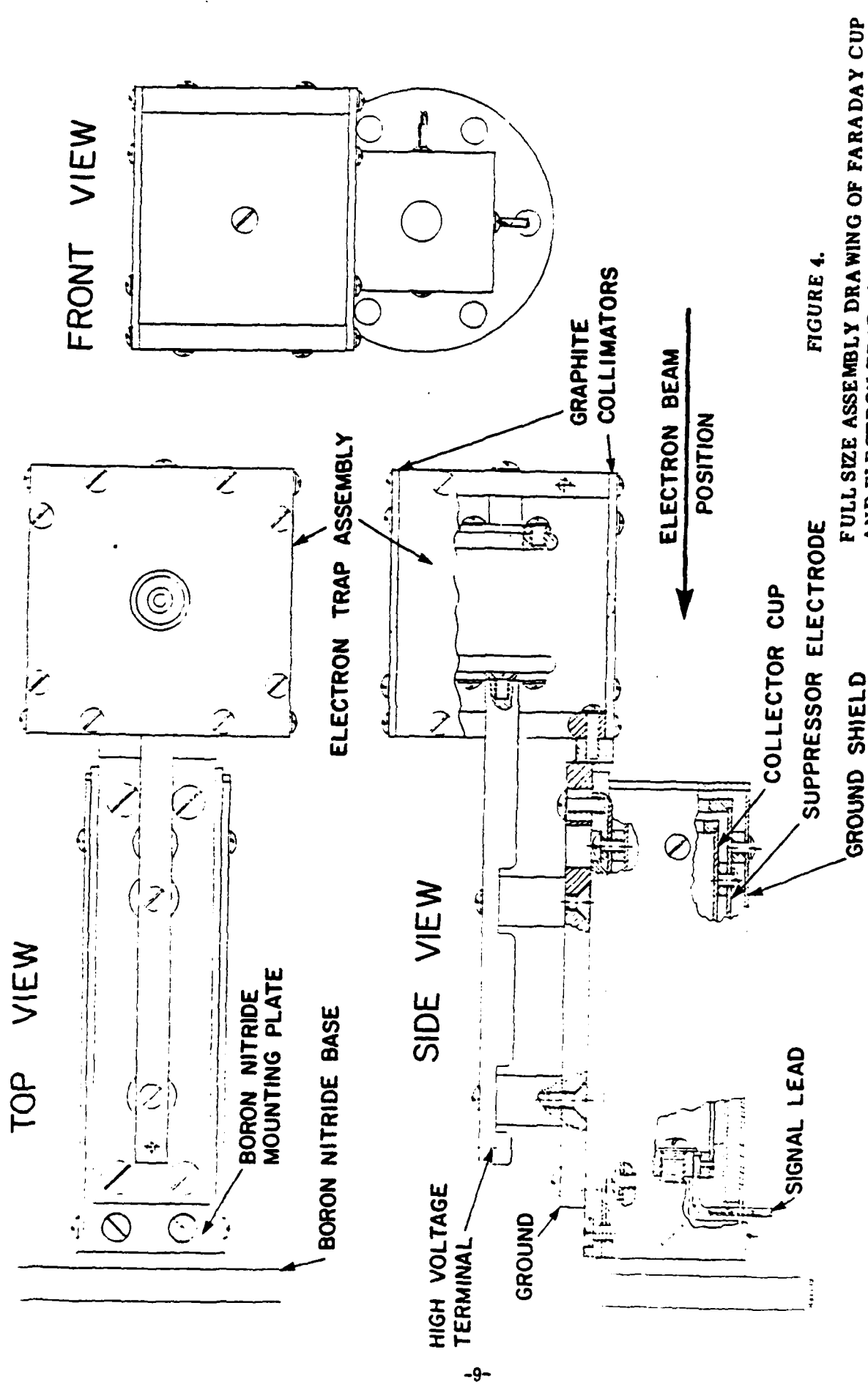


FIGURE 4.

FULL SIZE ASSEMBLY DRAWING OF FARADAY CUP AND ELECTRON TRAP (The collector cup, suppressor electrode and ground shield are all made with molybdenum sheet stock. Boron nitride was chosen for the insulator material due to its low outgassing characteristics.)

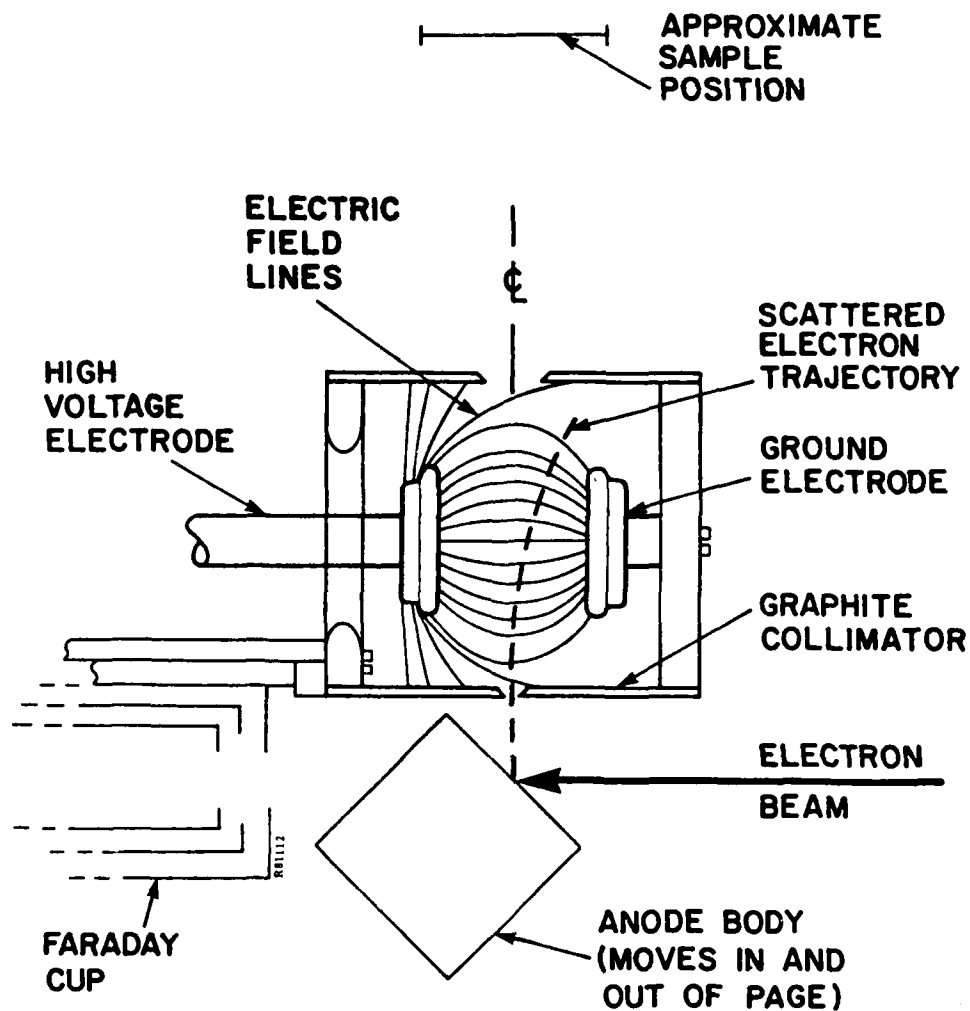


FIGURE 5. SCHEMATIC VIEW OF ELECTRON TRAP
(The electric field lines are approximate,
and are drawn to illustrate the effect of
the trap on a scattered electron. The
collimator holes have been designed to
produce a 3/4-inch diameter beam at the
sample position.)

one of the anode targets. The lower graphite collimator allows a certain fraction of these x-rays and electrons to enter the electron trap. The high voltage and ground electrode form a transverse electric field to sweep the electrons out of the beam of x-rays. An estimate for the transverse distance which these electrons are moved by such a field is as follows:

$$\begin{aligned}
 \text{Let } d_T &= \text{fixed distance between electrodes} \\
 V_T &= \text{voltage drop between electrodes} \\
 E_T &= V_T/d_T = \text{transverse electric field} \\
 qE_T &= \text{transverse force on electron} \\
 qVs &= \text{energy of scattered electron} \\
 S_T &= \text{transverse length electron travels due to } qE_T \\
 \Delta t &= \text{transit time of electron to pass through the electrode region}
 \end{aligned}$$

$$\text{Then: } S_T = \frac{1}{2} \frac{qE_T}{m} (\Delta t)^2 = \frac{1}{2} \frac{qV_T}{md_T} (\Delta t)^2$$

$$\text{and } \Delta t = \left(\frac{d_T}{2qVs} \right)^{1/2}$$

$$\text{Hence: } S_T = \left(\frac{V_T}{4Vs} \right) d_T$$

If the scattered electron has its original energy, and the potential applied to the electron trap is the accelerating voltage of the electron gun, then $V_T = Vs$ and $S_T = d_T/4$. For the present design, $d_T = 0.8$ inches, so that $S_T = 0.2$ inches. The parabolic curve drawn in Figure 5 illustrates this amount of transverse movement by a scattered electron entering the electron trap along the center line.

One could imagine a scattered electron which experiences a second scatter event at the collimator orifice, and leaves that scatter site heading in the direction of the high voltage electrode. The transverse electric field may deflect this electron, depending upon its kinetic energy, so that it exits the trap through the upper orifice. However, its trajectory would not be collinear with the center line and, because of the distance to the sample, there would be little chance of it striking the sample. Extra graphite baffles can be placed above the electron trap to capture escaping electrons if deemed necessary.

3.0 PRODUCTION OF X-RAYS

3.1 Estimated X-Ray Irradiance and PMMA Exposure Times

From Green and Cosslett's paper,⁽¹⁾ the x-ray radiation yield, generated by an electron beam impinging upon a solid thick target, is:

$$N_x = G (E_o - E_x)^n \quad (\text{quanta/electron})$$

where:

N_x	=	yield of x-rays per incident electron
G	=	generation efficiency factor
E_o	=	shell ionization energy (keV)
E_x	=	incident electron energy (keV)
n	=	1.63 (a constant)

For K_α and L_α characteristic lines, curve fitting of Green and Cosslett's data produced the relation:

$$G_{K\alpha} = 3.2 \times 10^{-4} \exp(-Z/10.92) \quad (\text{quanta/electron})$$

$$G_{L\alpha} = 8.5 \times 10^{-5} \exp(-Z/32.0) \quad (\text{quanta/electron})$$

The irradiance of a given target irradiated with 15 keV electrons is given by

$$I_s = \frac{N_x}{4\pi} \text{ Eph } (6.6 \times 10^4) \left(\frac{\mu W}{\text{Sr-W}} \right)$$

where:

Eph = characteristic photon energy in keV.

The irradiance, I_s , for five different target elements is tabulated in Table 1.

TABLE 1. X-RAY SOURCE IRRADIATION AND PMMA IRRADIATION TIMES

Target Element	Eph (keV)	GK α or GL α	Yield (# ph/e)	I_s ($\mu W/\text{Sr-W}$)	X-Ray Power on Resist ($\mu W/\text{cm}^2$)	PMMA Incident Sensitivity (J/cm^2)	PMMA Irrad. Time (Minutes)
Pd	2.84	2.0×10^{-5}	1.1×10^{-3}	15.9	71.6	3.65	850
Si	1.74	8.9×10^{-5}	5.9×10^{-3}	54.2	243.0	0.92	63
Al	1.49	9.7×10^{-5}	6.7×10^{-3}	52.6	237.0	0.59	41
Cu	0.93	3.4×10^{-5}	2.5×10^{-3}	12.2	54.9	0.16	49
C	0.28	1.8×10^{-4}	1.5×10^{-2}	21.8	98.1	0.12	21

If a 10 cm x-ray source-to-resist distance is assumed with 450 watts of electron beam power on the anode target, then the estimated x-ray power fluences on resist targets can be calculated. To estimate the time required to fully irradiate PMMA to a dose of 575 J cm^{-3} , the absorption coefficient curve for PMMA is required. This is plotted in Figure 6, the x-ray wavelengths noted for five elements. The major absorption edge in PMMA is, of course, the 284 eV K α edge of carbon. The PMMA sensitivity to a given x-ray energy is determined by dividing 575 J cm^{-3} by the appropriate absorption coefficient for that energy. With the x-ray power fluence on the resist and the sensitivity of the resist known, the required irradiation time using each target element can be calculated.

3.2 Experimental Check of Calculation

To check the calculations performed using the Green and Cosslett empirical formulation,⁽¹⁾ the results can be compared directly to experimental data for Al with the x-ray lithography facility built for the U. S. Air Force by Hughes Research. Sullivan⁽²⁾ measured the x-ray yield for an Al anode bombarded with 7 keV electrons using PMMA resist as a detector. The comparison is as follows:

	<u>Sullivan (7 kV)</u>	<u>Spire (15 kV)</u>
Yield (#ph/e)	1.53×10^7	6.7×10^{-3}
Irradiance (μ W/Sr-W)	12.9*	52.6

Using the Green and Cosslett formula for x-ray yield, the two yields listed above were calculated. The ratio $6.7/1.53 = 4.37$, when multiplied by the measured irradiance of $12.9 \mu\text{W/Sr-W}$, gives $56.3 \mu\text{W/Sr-W}$ as the comparison estimated irradiance for 15 kV. The Spire estimate of $52.6 \mu\text{W/Sr-W}$ for the irradiance of Al bombarded with 15 keV electrons is at least consistent with Sullivan's data.

3.3 Dosimetry

To aid the calculational efforts required for this contract, a Fortran program called NRLXRF has been ordered from COSMIC (Computer Software Management & Information Center, University of Georgia). NRLXRF, developed by John W. Criss of NRL, was created to aid in the analysis of x-ray fluorescence spectrometry data. One of its uses will be to predict characteristic x-ray line and bremsstrahlung intensities for most elements located in targets of varied composition, thickness, homogeneity, etc. The program incorporates physical theory and numerical methods to perform calculations employing one or the other, or both as needed. Phillip Blais (Westinghouse Research Center, Pittsburgh, PA) highly recommends NRLXRF as he has used it extensively for his studies.

*experimentally measured

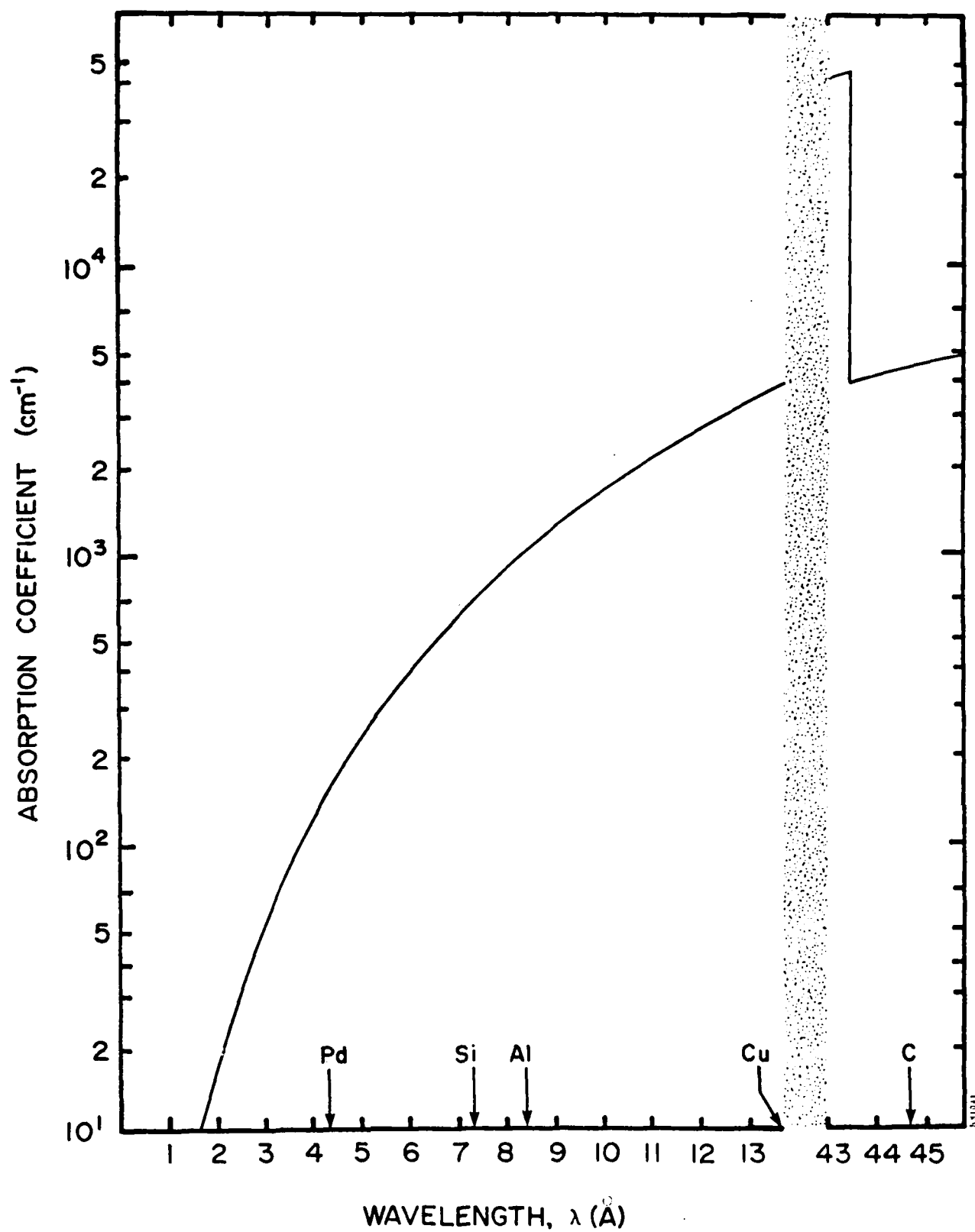


FIGURE 6. X-RAY ABSORPTION COEFFICIENT FOR
POLY(METHYL METHACRYLATE), $\text{H}_8\text{C}_5\text{O}_2$ PMMA

4.0 INITIAL MEASUREMENTS USING A RESIST MATERIAL

4.1 Electron Beam Evaporator

To produce low energy x-rays for the purpose of measuring dose profiles near high Z/low Z material interfaces, an electron beam evaporator unit is well suited. A Sloan E-beam evaporator unit, which is available for this work, has a 10 keV electron beam. The beam is deflected 270° before striking a water cooled solid metal target. This configuration is illustrated in Figure 7.

4.2 Photoresist Materials as Dosimeters

A number of resists could be used as x-ray dosimeters. All are hydrocarbon-based materials which have the same kind of x-ray energy absorption (see Figure 6). The detector chosen for these experiments will be a positive electron beam resist called PBS (Poly(butene-1 sulfone))(3). This resist was chosen because of its high sulfur content which enhances its sensitivity to Ag L_{α} radiation. PBS, like other organic resists, behaves as: (4)

$$\chi = K D^{\beta}$$

where χ is the dissolution rate (nm/min), K and β are constants, and D is the dose (J/cm³). Its behaviour over the dose range of 10-50 J/cm² is nearly linear as shown in Figure 8(5). This implies that spatial variations in surface dose will result in initial etch rates which vary, above a threshold dose D_c of about 10 J/cm³, nearly linearly with $D - D_c$.

It needs to be stated explicitly that such an x-ray dosimeter cannot be used in any absolute sense. Rather, its primary use would be as a working dosimeter to monitor dose from one experiment to the other. With an optimized, standard resist handling protocol (spinning, prebake, storage, irradiation, development), PBS is be a very useful x-ray dose monitor.

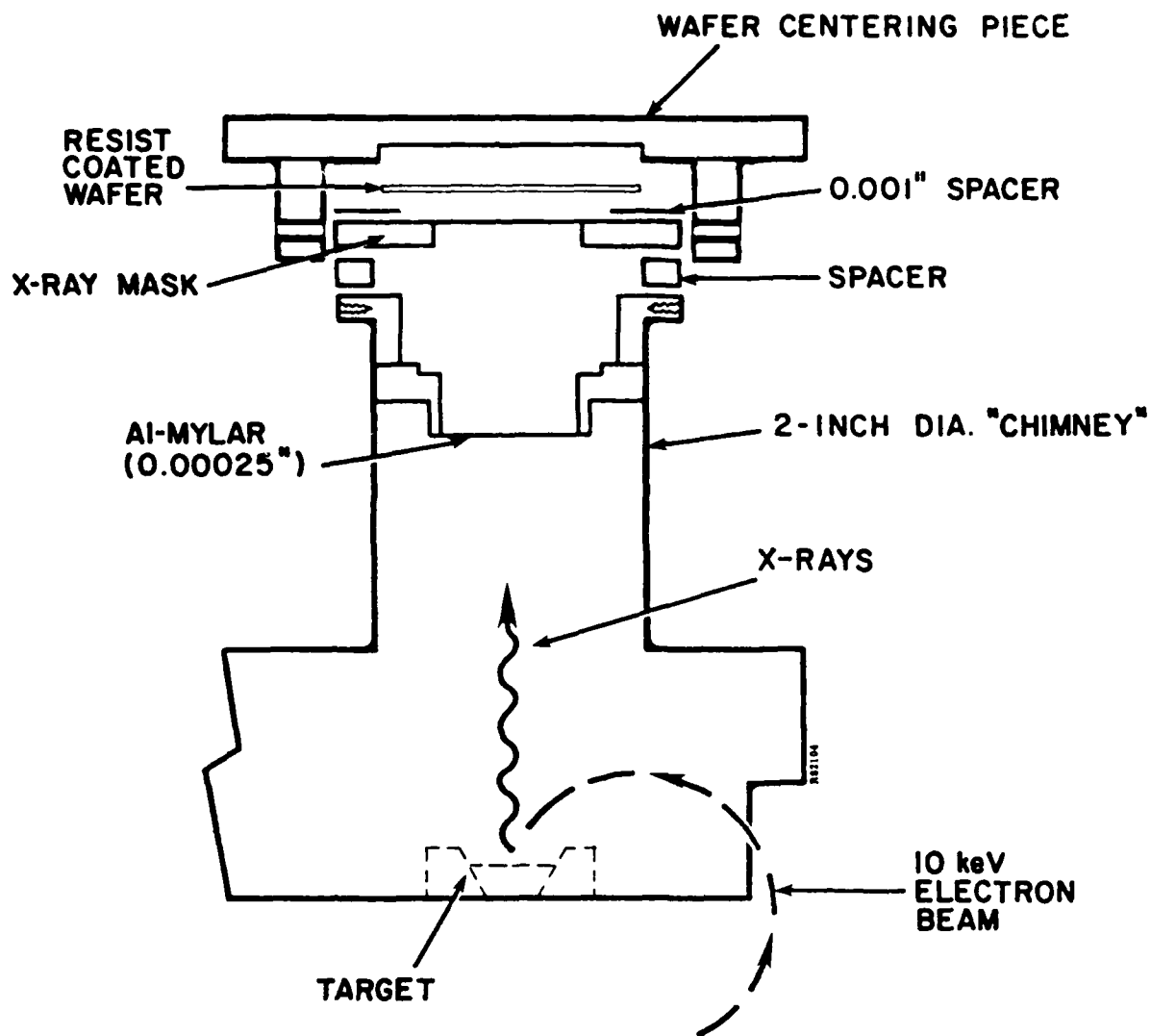


FIGURE 7. E-BEAM EVAPORATOR APPARATUS FOR X-RAY IRRADIATIONS

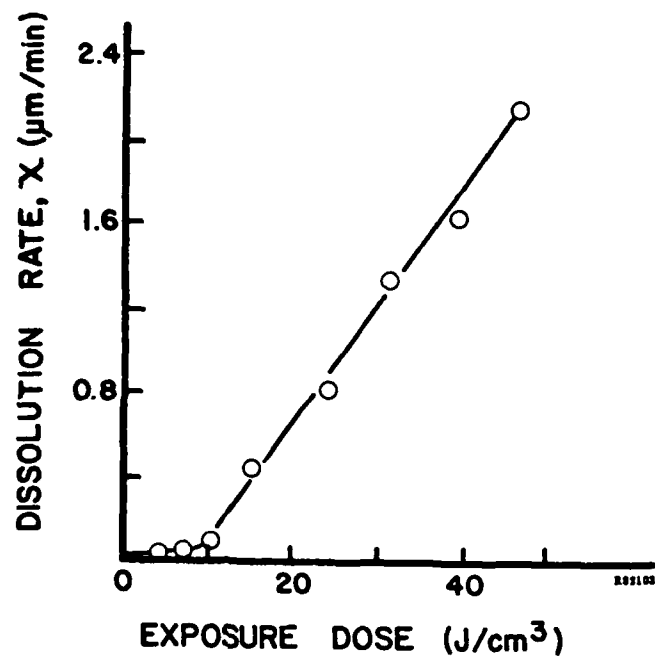


FIGURE 8. CHARACTERISTIC EXPOSURE CURVE FOR PBS USING $\text{Ag } L_{\alpha}$ RADIATION.

4.3 X-ray Irradiation of PBS

Figure 9 shows the x-ray absorption coefficient curve for PBS. The K-edge absorption peak shown is due to the sulphur in this material. Note that while the silver Ag L_{α} radiation is approximately twice the energy of the Al K_{α} irradiation, its absorption in PBS is about 60% of that for Al. The sulphur incorporated into PBS raises the sensitivity of the material for these higher energy x-rays by about a factor of 4.

Using the x-ray absorption coefficient curve (Figure 9) and the PBS characteristic exposure curve (Figure 8), the exposure times required to fully irradiate PBS at different x-ray energies can be calculated. Table II gives the pertinent data to calculate the estimated irradiation times. Note that the calculated exposure times are based on an assumed 200 W of electron beam power on the target and a target to resist layer distance of 15 cm. From these numbers it appears that Ni would not be a likely candidate for our planned experiments due to the large exposure time required. This time is due to two factors: 1) the relatively low energy of the incident electrons (10 keV) and, 2) the relative insensitivity of the PBS material to the Ni radiation. If the electron beam energy could be raised to 20 keV, then the K_{α} radiation for Ni would increase by a factor of 24, reducing the exposure time to 2.8 hours.

Table II
X-ray Irradiation of PBS Data

Element	X-ray Energy (keV)	E (keV)	G (10^{-5})	Yield (ph/e $^{-}$) (10^{-4})	X-ray Power (μ W/Sr-W)	Power* at Resist (μ W/cm 2)	PBS** Sens (mJ/cm 2)	Exp Time (min)
Al	1.49	1.56	9.7	3.1	24.2	20.8	16.6	13.3
Pd	2.84	3.60	2.0	4.1	6.1	5.2	28.5	91.3
Ag	2.98	3.80	1.96	3.8	6.0	5.1	33.3	108.
Ti	4.51	4.96	4.3	5.9	14.0	12.0	117.	2.7h
Ni	7.47	8.33	2.5	0.58	2.3	1.98	500	69h

* Power delivered to resist surface for a 200W electron beam power level on target and a target-resist distance of 15 cm.

** Based on a sensitivity value of 20 J/cm 3 for PBS.

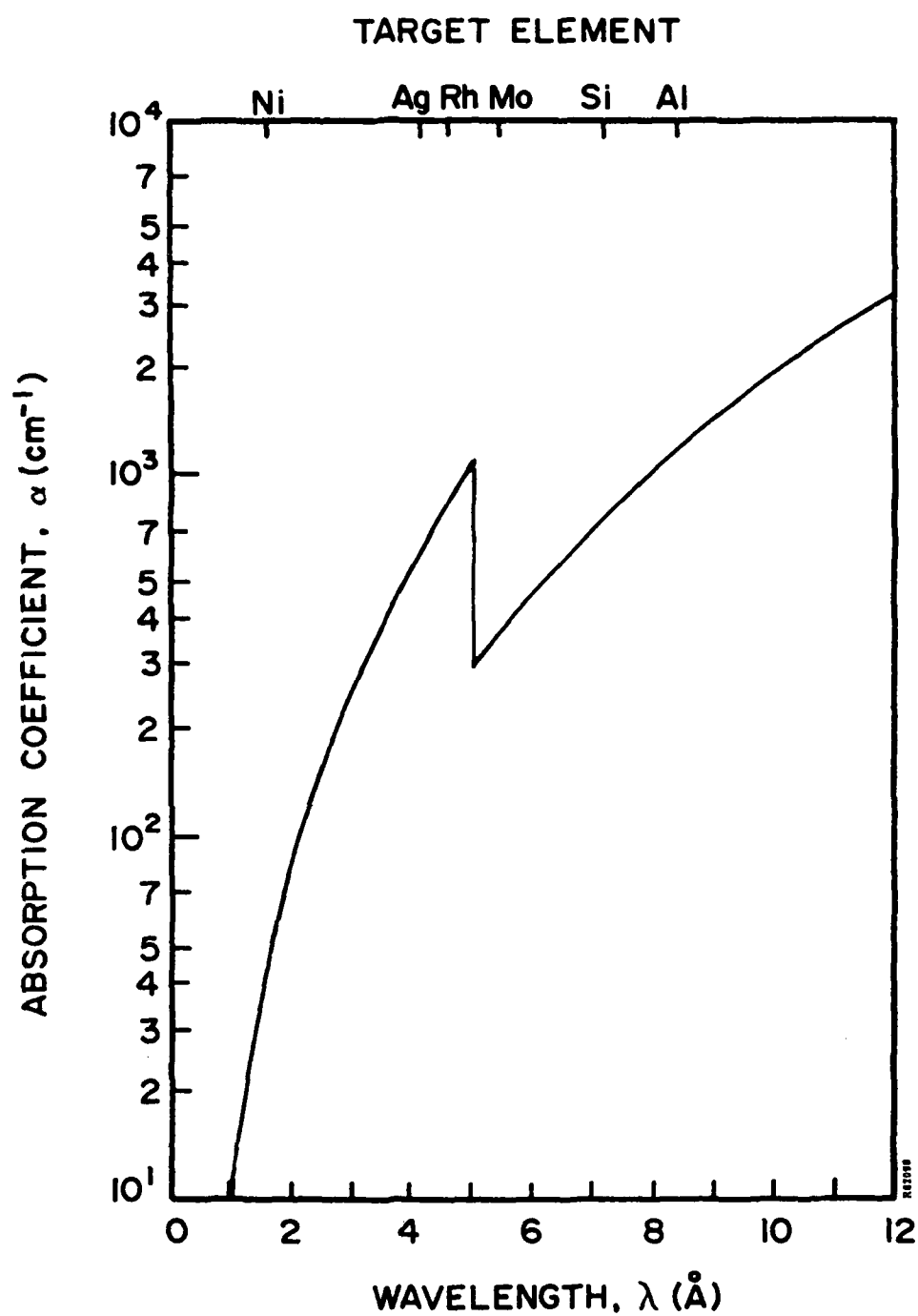


FIGURE 9. X-RAY ABSORPTION COEFFICIENT AND TRANSMISSION FOR POLY(BUTENE-1-SULFONE) RESIST.

4.4 Poly (Butene-1 Sulfone) (PBS) Resist as a Detector

Four ounces of this material with developer and rinse solutions were purchased from KTI Chemicals (Wallingford, CT). Since this material is proprietary (Bell Telephone Laboratories, Princeton, NJ), user information is sparse. Brian Murray traveled to Hunt Chemical (East Providence, RI) to work with Mr. Medhat Poukhey to learn how to best spin coat Si wafers with this material and to understand its development characteristics.

Since PBS is a non-viscous material with less than 4% solids, spin speeds during coating need to be kept fairly low if a thick layer is desired. It was found that the most uniform coatings were obtained by first flooding the wafer while stationary with resist material and then turning on the spinner with a ramp acceleration to reach its pre-set speed. Coating speeds of 1000 rpm, 1500 rpm, 2000 rpm, and 3000 rpm were tried. The 3000 rpm coated wafer appeared to be spotty and streaky in spots, due to a very thin layer of material. The pre-bake temperature used was 120°C for 30 minutes⁽⁵⁾ After the pre-bake, a small scratch was made in the resist layer of each wafer so that Dektac thickness measurements could be done. Figure 10 illustrates the measurement data for the 1000 rpm and 3000 rpm cases. Since 1000 rpm on most wafer spinners is the minimum speed, resist thickness in the range of 3500 Å will be the thickest resist layer obtainable with this material. The application of a second layer over the first layer was attempted, but little was added to the thickness of resist on the wafer. This was probably due to the fact that the resist solvents dissolved the first layer during the spin coating of the second layer.

4.5 Experiments with An X-ray Mask

A mask, with the Air Force 1951 pattern, was kindly given to us by Mr. Phillip Blais from Westinghouse Research Center, (Pittsburg, PA). Its substrate is 6 microns of polyimide and the high Z absorber is gold with a thickness of 6000 Å. Figure 7 illustrates the experimental apparatus used to obtain the x-ray mask patterns on a PBS coated wafer. A 0.001 inch thick Mylar spacer was placed between the wafer and the mask. The 0.00025 inch thick aluminized Mylar is used to absorb electrons which scatter from the target and to help reflect the infrared radiation that is generated from the target itself.

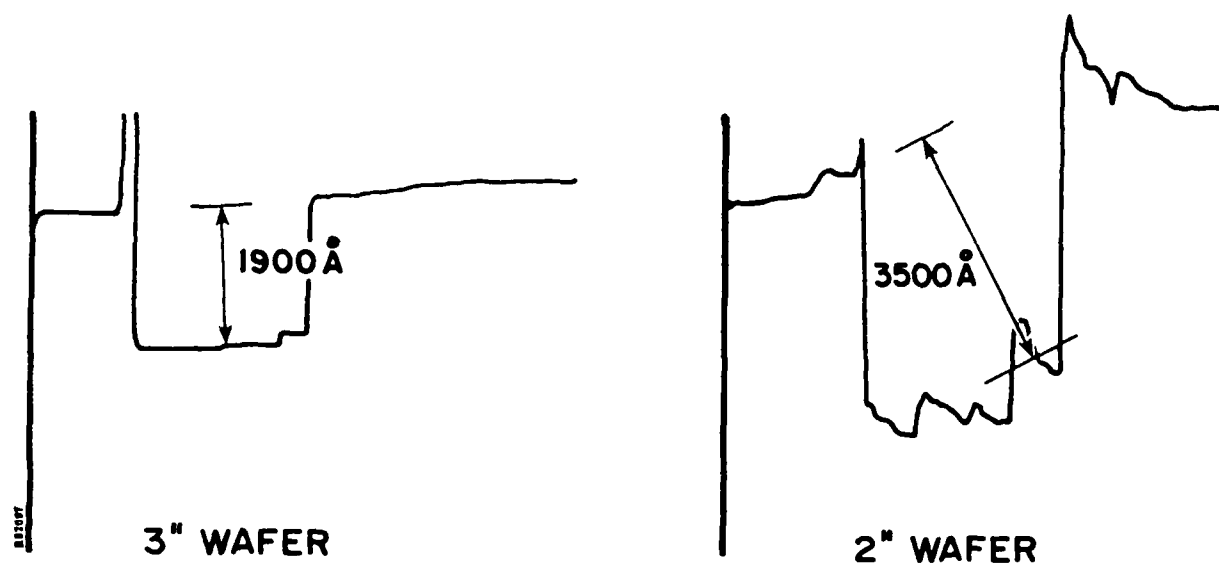


FIGURE 10. DEKTA THICKNESS MEASUREMENTS OF PBS SPUN COATINGS ON Si WAFERS (Spun at 3000 rpm (left) and at 1000 rpm (right)).

The two targets used for the initial experiments were Al and Ag. By experimentation it was determined that 80 mA of electron beam could fall on the Ag target before melting occurred and about 40 mA could be used for the Al target. This means that the electron beam power on target for Ag is about 800 watts and for Al about 400 watts. However, the Al-Mylar electron/heat shield does absorb some x-rays, so that taking the irradiation time in Table 1 and dividing by the appropriate electron beam power factor does not take into account the absorption in this shield material. As a result of this, it was decided to use a 45 minute irradiation for the Ag target and a 10 minute irradiation time for the Al target.

Figure 11 illustrates a masked pattern developed on a PBS coated Si wafer. The wafer was coated with a 2700 Å thick layer of PBS. The development time was 20 seconds. Regions of the resist which were not under the gold absorber were completely removed in this 20 second development time. The pattern seen in Figure 11 is the gold absorber pattern on the mask. It appears that some overdevelopment did take place as these resist regions appear somewhat speckled.

5.0 DOSE PROFILE MEASUREMENTS USING PBS RESIST

5.1 Rationale for Experimental Approach

The rationale for the experiments performed may be described as follows. By using Au as the high Z material, a measurement of the dose profile (produced by soft x-rays) in a low Z material adjacent to the Au can be carried out using various thicknesses of low Z absorbers. If the dosimeter material (PBS) is placed adjacent to the low Z absorbing layers, various dose levels will result in the dosimeter according to the absorber thickness. In this way, dose levels varying with low Z absorber thicknesses are determined and, as a result, a dose profile is measured.

Ideally, if PBS is the dosimeter, the low Z absorbing layers on the Au should be PBS as well. However, since thicknesses of the order of 100 Å are anticipated for the determination of a dose profile, carbon is a more practical first choice for the low Z absorbing material. dose profiles can be found for the material configuration Au:C:PBS. To a first approximation, carbon and PBS are considered as a single material.

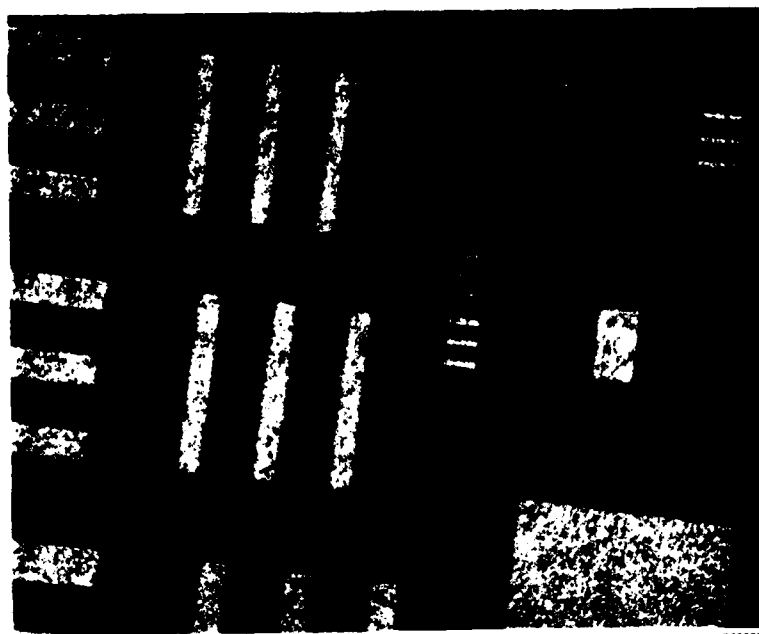


FIGURE 11. DEVELOPED X-RAY MASK PATTERN USING PBS. (The Smallest Bar Length Is Shown About 10 Microns. The Dark Regions Are Bare SiSubstrate.)

5.2 High Z/Low Z X-ray Masks

To make appropriate material interfaces for these experiments, very thin material layers are required. A convenient substrate material is 2.5 micron thick mylar suspended on a 1-inch diameter circular frame. This object is called a pellicle and is available from the National Photocolor Corporation (Mamaroneck, NY). A layer of Au is first evaporated onto the mylar to a preselected thickness. Carbon, is then evaporated onto different regions of the Au layer to various thicknesses. Placing the detector material, PBS resist, which has been spun as a thin film onto a silicon wafer, next to the Au/C interface then completes the experimental configuration. Some regions of the PBS will be next to the mylar only, some regions next to the gold only, and a number of regions next to the variously thick layers of carbon. Figure 12 illustrates the experimental configuration for these studies.

5.2.2 Metal Evaporation

Mr. Joe Lorenzo of Hanscom Air Force Base carried out the metal evaporations onto the mylar pellicles for these experiments. Three separate evaporation runs were performed, two for gold and one for silver. A crystal oscillator rate deposition monitor was used to measure the deposition rate of the gold or silver during each evaporation run. A glass slide, placed in the evaporator at the same distance from the evaporation source as the pellicle, served as an independent monitor of the metal thickness evaporated on the pellicle.

Figure 13 shows the Dektak measurements of the Au and C layers of the first mask used in these experiments. Figure 13 shows the measurement on a glass slide of the Au thickness (6800 Å) which was deposited on the mylar pellicle. In Figure 14, the Dektak measurements are shown for the deposited silver layer. The Ag evaporation was carried out in two separate runs because the silver charge in the evaporation boat ran out after 1500 Å was deposited. The chamber had to be opened up and a new silver charge placed in the boat. The figure shows two measured thicknesses, one of 1500 Å and the other of 2000 Å, measured on two separate glass slides. The sum is the Ag layer deposited on the pellicle surface. The third thickness measurement (Figure 14C) is that of the silver on the pellicle itself. This was done by placing the pellicle on a 1-inch diameter Si wafer supported by a machined Al support. The Dektak measurement on the pellicle surface

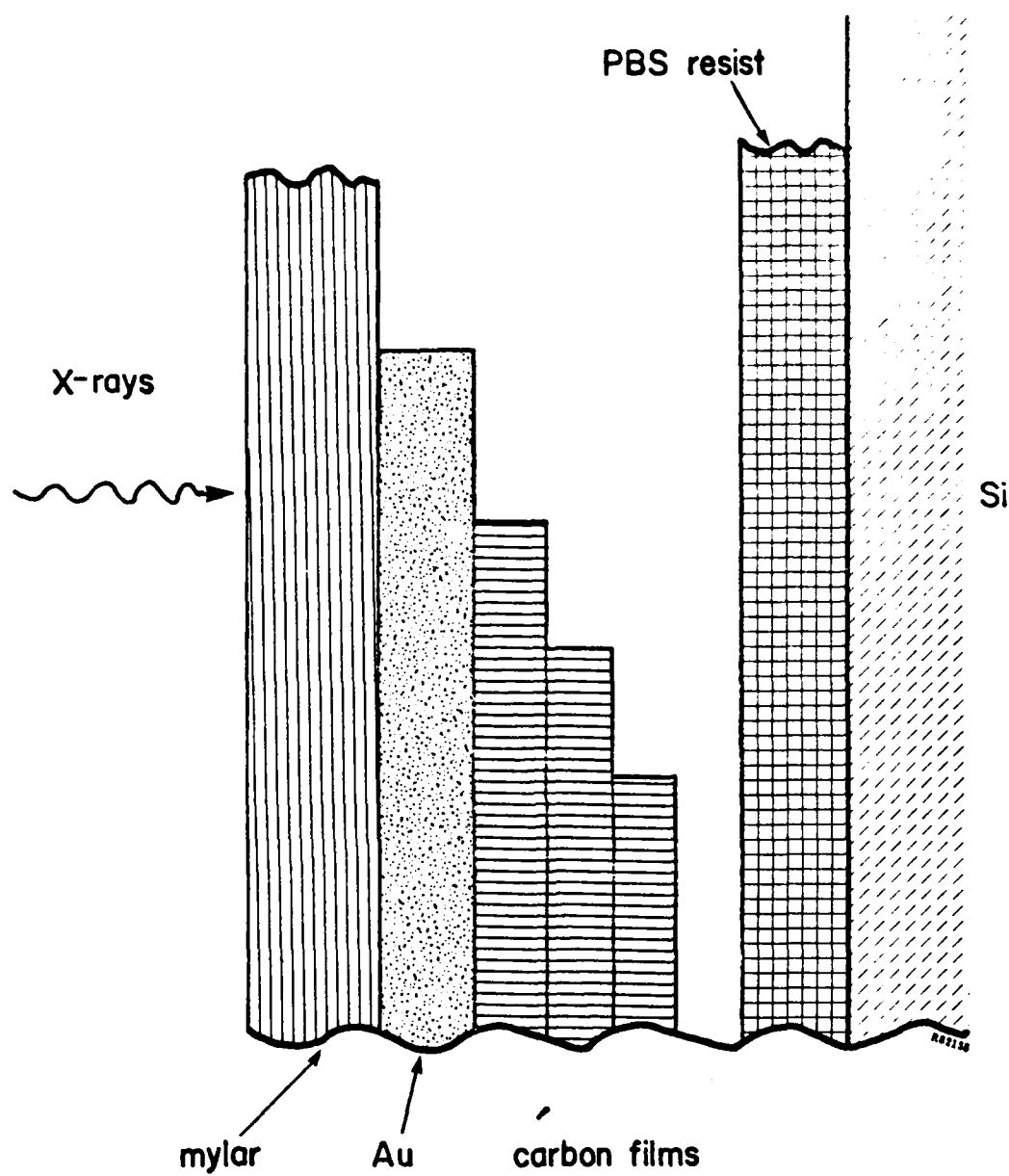


FIGURE 12. EXPERIMENTAL CONFIGURATION FOR MEASURING DOSE PROFILES NEAR Au/C INTERFACE.

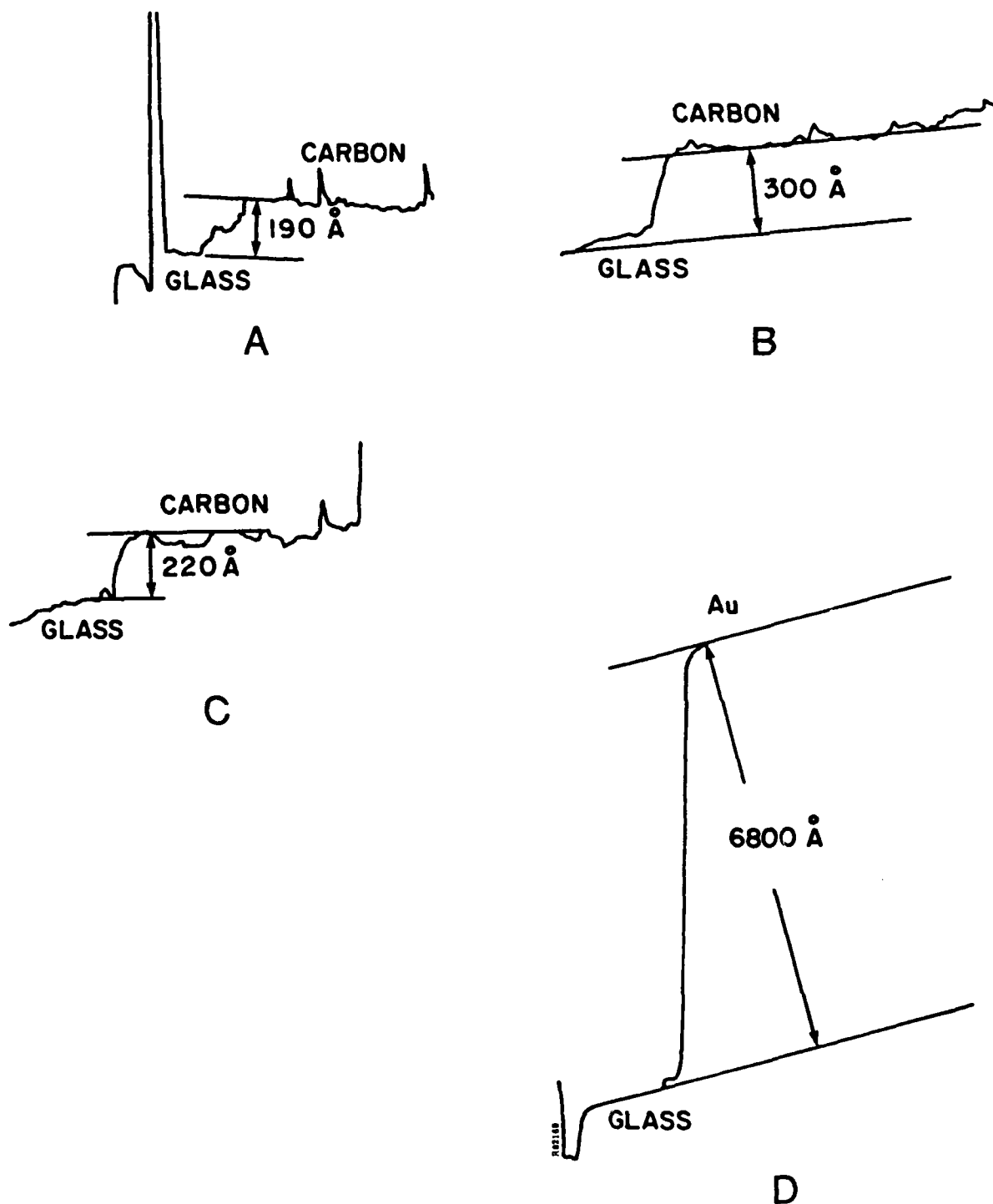


FIGURE 13. DEKTAK MEASUREMENTS ON GLASS OF CARBON AND Au LAYER THICKNESSES. (A, B and C are the three layers of carbon laid down on the Au absorber for the first Au/C mask used.)

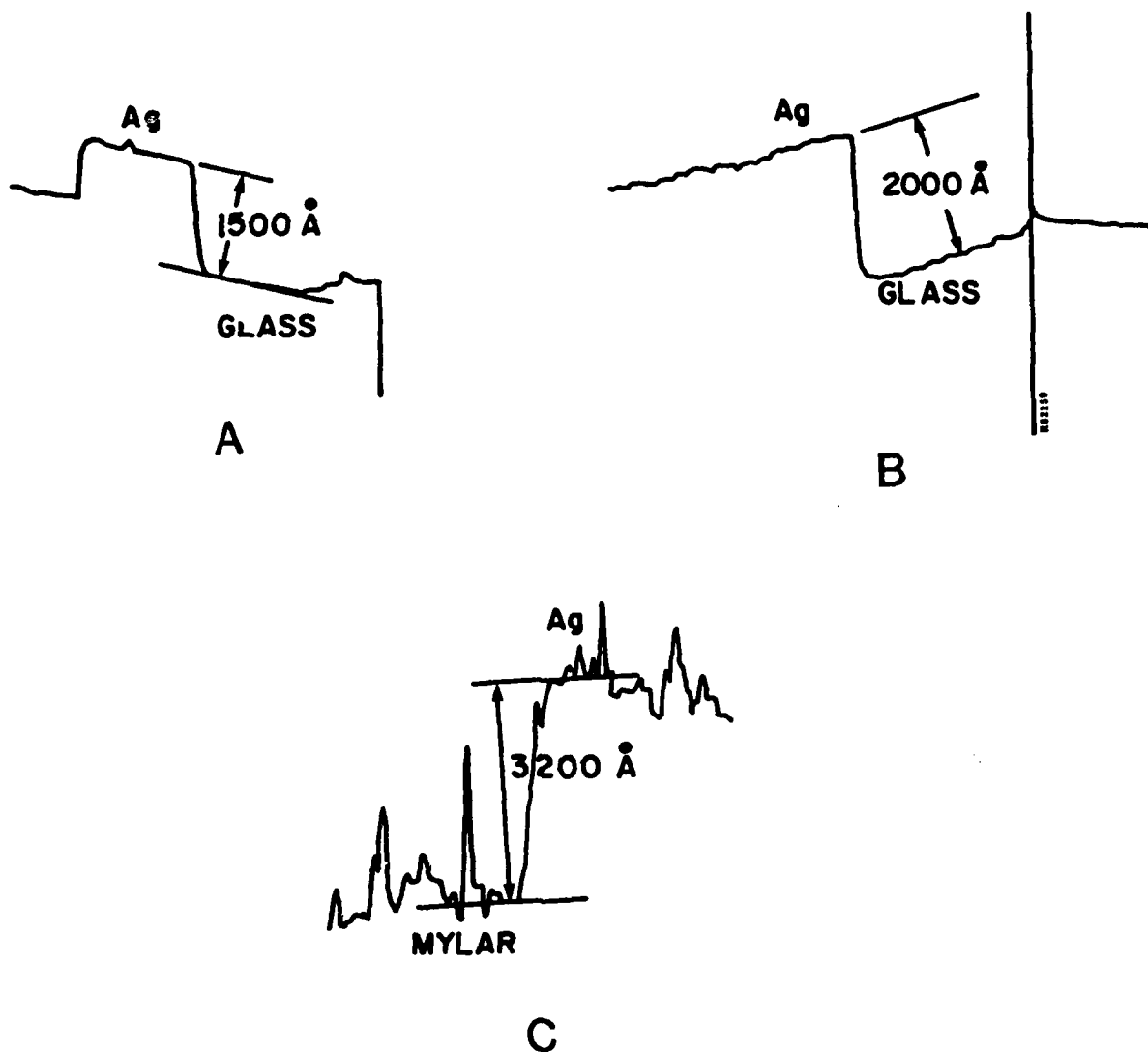


FIGURE 14. DEKTAK MEASUREMENTS OF THE Ag EVAPORATION ONTO MYLAR PELLICLE. (A and B are measurements of the evaporation monitor glass slides. C is a measurement of the total Ag thickness of the pellicle itself.)

showed a rough Ag surface. This roughness prevented a precise measurement of the carbon layers that were subsequently laid down on the silver surface.

5.2.3 Carbon Deposition on X-ray Masks

Mr. Joe Comer of the Hanscom Air Force Base carried out the carbon deposition runs for this program. The apparatus consists of an evacuated bell jar, two pointed graphite rods in near proximity, the pellicle to be coated behind a mask, , and two glass slides to monitor the deposited carbon thickness. Since no deposition rate monitor was available for the carbon coatings, an oil coated glass slide acted as a visual indicator for the thickness of carbon being deposited during a run. The 6800 Å gold coated pellicle was used for the first run. The vacuum in the evaporator unit was about 2×10^{-5} torr, pumped with a liquid nitrogen cold trapped diffusion pump. For each run, the carbon arc source which creates the deposited carbon lasted generally for three to five seconds.

5.2.4 Gold/Carbon Mask

Figure 13 shows the Dektak measurements made on the monitor glass slides for each carbon deposition run for the first Au/C mask. The three thicknesses were measured to be 190 Å, 300 Å and 220 Å. In an independent kind of measurement, Mr. Joe Comer determined the second carbon thickness using a stereomicrometer parallax measurement of electron micrographs. This is a rather delicate technique in which a carbon film is floated from a glass slide upon which it was originally deposited and coated on both sides with a very thin layer of gold. An electron micrograph is then taken using an electron microscope. The micrograph is then viewed with stereographic eyepieces. The result of this measurement is 313 ± 30 Å. This is in very good agreement with the Dektak measurement of Figure 13B.

In addition to the three carbon films laid down on the Au (Figure 13) there was also a small area of carbon (deposited next to the 220 Å thick area) which has a thickness of about 100 Å. The final parameters of this first experimental mask are listed in Table 3.

Table 3. X-ray Mask Parameters

Material	Thickness	Diameter
Mylar	2.5 microns	2.54 cm
Au	6800 Å	1.60 cm
C	100 Å	—
C	220 Å	1.35 cm
C	520 Å	1.1 cm
C	710 Å	0.65 cm

The complete mask is shown in the upper left of Figure 15. The "pac-man" configuration of carbon layers on the Au was meant to place bare Au next to each carbon layer thicknesses. All the C layers are not visible in this photograph. Figure 15A is a photomicrograph of this mask showing portions of the bare Au, the 100 Å and 510 Å carbon layers.

5.2.5 Silver/Carbon Mask

The carbon layer deposition on silver mask was performed using a different mask arrangement, one in which seven separate carbon depositions on the silver were carried out. The carbon layer configuration for the silver mask is also shown in Figure 4. Unfortunately, the glass slide monitor approach for this case was faulty. Basically, a single glass slide was used whereby only a small portion of the glass slide was exposed to the carbon deposition for each run so that a step wedge of carbon layering was established on the glass slide. However, Dektak measurements of this set of carbon layers gave inconsistent results so that the carbon thicknesses laid down on the silver mask cannot be adequately established. Attempts to measure the carbon layer thicknesses directly on the pellicle could not be done due to the severe roughness of the Ag and, presumably, the mylar as well. The photomicrograph in Figure 16B illustrates this roughness very well.

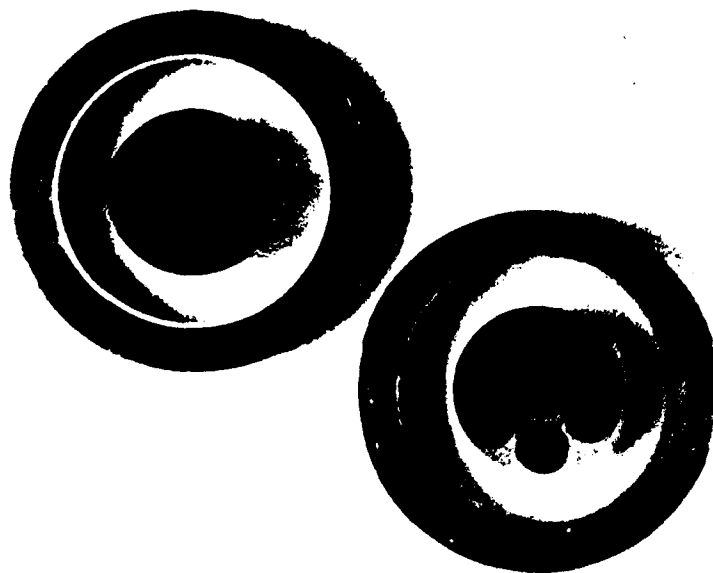
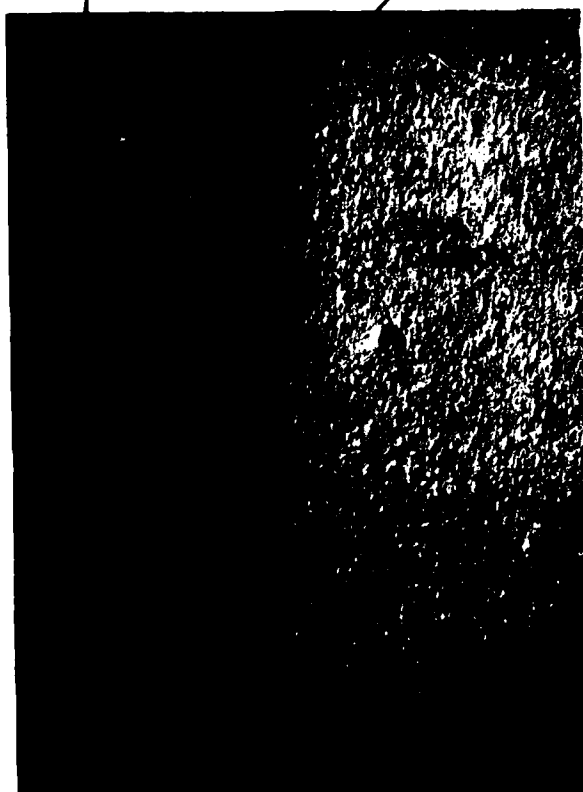


FIGURE 15. PHOTOGRAPH OF THE Au/C AND Ag/C X-RAY MASKS.

510 A CARBON

BARE Au



A



B

FIGURE 16. NOMARSKI (DIC) PHOTOMICROGRAPH OF SELECTED REGIMES OF THE EXPERIMENTAL X-RAY MASKS: A - Au/C MASK AND B-Ag/C MASK.

5.2.6 Spinning of the PBS Resist on Silicon Wafers

The coating of PBS resist on cleaned silicon 2" diameter wafers generally resulted in coating thicknesses in the range of 2600-3500 Å. Low spin speeds of 1000 rpm are necessary to obtain this thickness of PBS coatings. A number of problems have been encountered in the PBS resist spinning. These include streaks and various other kinds of defects in the coating. It was thought that high humidity in the room in which the resist was being coated may be a factor in its poor coating performance. As a consequence, a number of wafers were coated in a humidity controlled environment. These coated wafers appeared to have significantly fewer defects than those coated at Spire Corporation and were subsequently used for experiments.

5.2.7 X-Ray Irradiations

The Sloan multi-target, electron beam evaporator unit was again used as the x-ray source for these experiments. The apparatus to hold the wafer and mask is basically the same as sketched in Figure 7. For these experiments, the mask pellicle is placed facing upward at a distance of 15 cm from the x-ray target. A coated wafer is laid down on top of the pellicle and makes surface contact with the carbon and gold (silver) of the mask.

Three different characteristic x-ray sources are used with characteristic energies of 1.49 keV, 2.98 keV, and 4.51 keV. However, for a complete evaluation of these experiments, the bremsstrahlung component for each x-ray source needs to be carefully considered.

For the three x-ray targets used, the maximum electron beam currents that did not result in any surface melting were 40 ma for Al, 80 ma for Ag and 10 ma for Ti. The low current for the Ti is due to its low specific heat and low thermal conductivity to the water cooled target support. The electron beam striking the target was not a circular spot but, rather, a broad line of approximately 1 cm x 1 mm. Since only one dimensional dose profiles are being measured in these experiments, the broad electron beam on the target was not considered a significant problem. The vacuum level during each radiation run was in the range of 2×10^{-6} torr. After each irradiation, the apparatus was allowed

to cool down before venting the chamber with nitrogen gas. Use of the Ag and Ti targets produced significant heating to the experimental apparatus above the target. For both, a mask pattern was easily observed on the coated wafer after irradiation and before development. This is probably due to the heat which was generated from the target and transmitted through the aluminized mylar heat shield and the mask to the resist on the wafer.

5.2.8 Resist Development

For each irradiated wafer, the same development procedure was employed. The wafer was placed in a 2 inch diameter wafer holder, placed in the developer solution for ten seconds, taken out and shaken off once, then placed in the rinse solution and softly agitated, for 60 seconds. After this, the wafer was gently blown dry with dry nitrogen gas. In all cases with the Au/C mask, a pattern was observed on each irradiated wafer.

6.0 MEASUREMENTS AND RESULTS OF DOSE PROFILES

6.1. Ellipsometer Measurements

After the development of the exposed PBS-coated wafers, the dose data is contained within the thicknesses of each rather thin PBS layers. To measure such layers, an ellipsometer measured. The ellipsometer measurements were done using a Rudolph Research Auto EL III ellipsometer. The light source used is an He:Ne laser which puts out light with a wavelength of 6328 Å. The basic equation of ellipsometry can be stated as

$$\rho = (\tan \Psi) e^{i\Delta}$$

where ρ is the ratio of the complex reflection coefficients of the incident and reflected light from the sample, $\tan \Psi$ is the ratio of the real to imaginary reflection coefficient magnitudes, and Δ is a difference in phase of the two beams.

Nulling ellipsometers, such as the Auto EL III, generally employ a polarizer, an analyzer, and a compensator, each of which is aligned along the axis in which it is located. The polarizer is located in the incident beam axis the analyzer is located in the

reflected beam axis and the compensator is located in the incident beam axis. A compensator is fixed at some azimuthal angle with respect to the plane of incidence while the other two components are rotatable automatically during the measurement period. The measurement consists of setting an angle of incidence, usually 70° , with respect to the sample which is mounted with its surface at the intersection of two axis. The polarizer and analyzer are then rotated alternately until the intensity of the reflector beam is reduced to a minimum (as sensed by the photodetector). At that null condition, the angular azimuthal angle of the polarizer and the analyzer are determined. These two measured angles are directly convertible by simple linear equations into the polarization parameters Ψ and Δ . Once Ψ and Δ are determined, a simple computer program is used to determine the index of refraction and thickness of the transparent film on the silicon substrate. If the film is absorbing, however, it is not possible to determine uniquely the index of refraction and thickness from a single Ψ and Δ measurement with the presently available software from the manufacturer.

Figure 17 is a graphical representation of the Ψ and Δ that would be measured for transparent films of arbitrary thickness and refractive index on silicon substrate by the ellipsometer using a light source of wavelength 6328 \AA and at an angle of incidence of 70 degrees. Each line in the family of closed curves is the locus of the Ψ and Δ produced by films of increasing thickness but constant refractive index. All curves of constant refractive index must go through a single point, the Ψ and Δ coordinates of the bare silicon substrate. Intuitively, this must be so, since Ψ and Δ for all film covered surfaces, must approach the Ψ and Δ of the substrate as the films get thinner and thinner. Similarly, as the films get thicker and approach the cycle thickness, the Ψ and Δ again must approach the Ψ and Δ coordinates of the bare substrates because, at the cycle thickness, the film/substrate system behaves as if no film is present. For the PBS resist, the index of refraction has been measured to be about 1.53 , and this gives a cycle thickness of about 2620 \AA . In measuring various resist thicknesses on silicon, therefore, one needs to know an approximate film thickness as the ellipsometer will only measure between $0 - 2620 \text{ \AA}$, or $2620 \text{ \AA} - 5240 \text{ \AA}$, and so on. As an experimental consideration, the

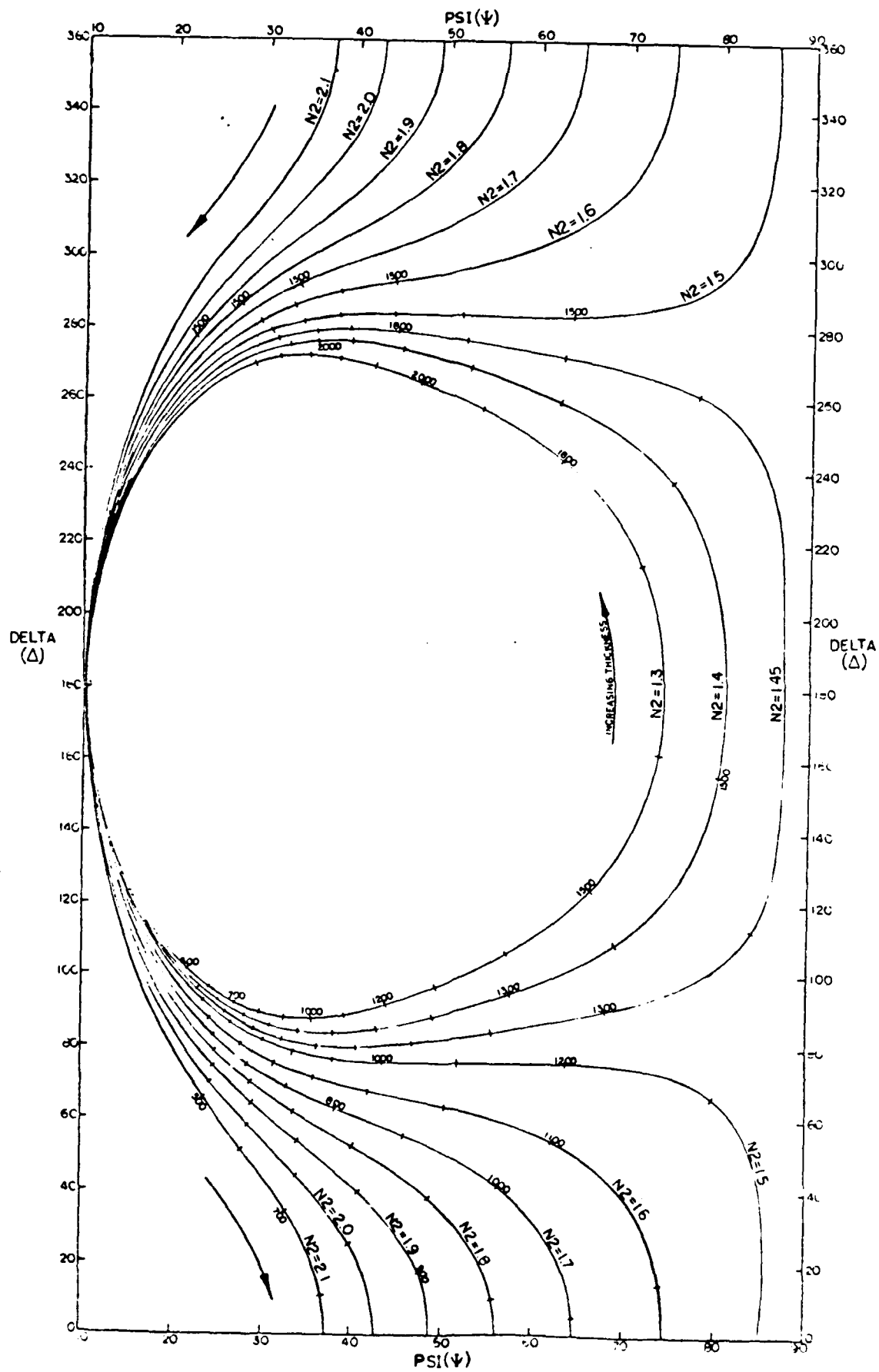


FIGURE 17. Ψ AND Δ VS. REFRACTIVE INDEX AND THICKNESS OF TRANSPARENT FILM ON SILICON SUBSTRATES. (Wavelength is 6328 Å.)

ideal resist thicknesses to be measured should vary between one-third and two-thirds the cycle thickness which, in the case of PBS resist, would be approximately 870 - 1740 Å. Very thin PBS resist films or those near the cycle thickness often lead to a null result in the measurement process.

6.2 Measurement Results

Typical ellipsometry data is illustrated in Table 4. The ellipsometer gives, for each reading, a value for Ψ , Δ , the index refraction, and the thickness of the film above the silicon substrate. The last column is the thickness difference between the unexposed resist region for each wafer and the various measured thicknesses. Plotting this column against the thickness of carbon in the first column will be a measure of the dose profile through the carbon material. Note that, for each measured wafer, the index of refraction stays fairly constant throughout the measurement of the different regions on that wafer.

The dose profile data is plotted in Figure 18. The Ti data is shifted upwards for convenience of display, and the Ag source profile curves are from data not listed in Table 4.

6.3 Comment on Dose Profile Data

The data shown for the Al K_{α} case would appear to be fairly easily explainable. The 1.49 keV X-rays from the aluminum source produce a dose enhancement next to the gold interface (0 carbon thickness) which is fairly readily absorbed in about 200 Å of carbon. As we move up in energy to the Ag L_{α} case, the dose profile definitely reaches no asymptote, but appears to continue downward as the carbon thickness reaches 710 Å. In fact, the silver data looks remarkably similar to the Ti K_{α} data and this is somewhat surprising. The titanium X-ray is 4.5 keV, about 50% greater than that for silver, yet the dose profile appeared to be similar in shape. What is missing, and not accounted for by our theoretical analysis to date, is the potential presence of bremsstrahlung in the X-ray sources.

Table 4
Typical Ellipsometer Measurement Data

Region	Δ	Ψ	Al K_{α} (6/7/82)		
			INDEX	THICKNESS (A)	DIFF (A)
Unexp. Resist	276.9	28.24	1.525	1989	0
Au	284.4	36.36	1.526	1776	213
100A	283.9	35.20	1.527	1801	188
220A	282.2	32.88	1.525	1860	129
520A	282.7	33.40	1.526	1845	144
710A	281.8	32.32	1.527	1870	118

Region	Δ	Ψ	Ti K_{α} (6/7/82)		
			INDEX	THICKNESS (A)	DIFF (A)
Unexp. Resist	73.84	43.76	1.523	982	0
Au	84.44	27.40	1.518	620	362
100A	82.80	28.64	1.515	657	325
220A	81.68	29.56	1.513	684	298
520A	78.84	31.92	1.518	747	235
710A	77.56	33.56	1.518	790	192

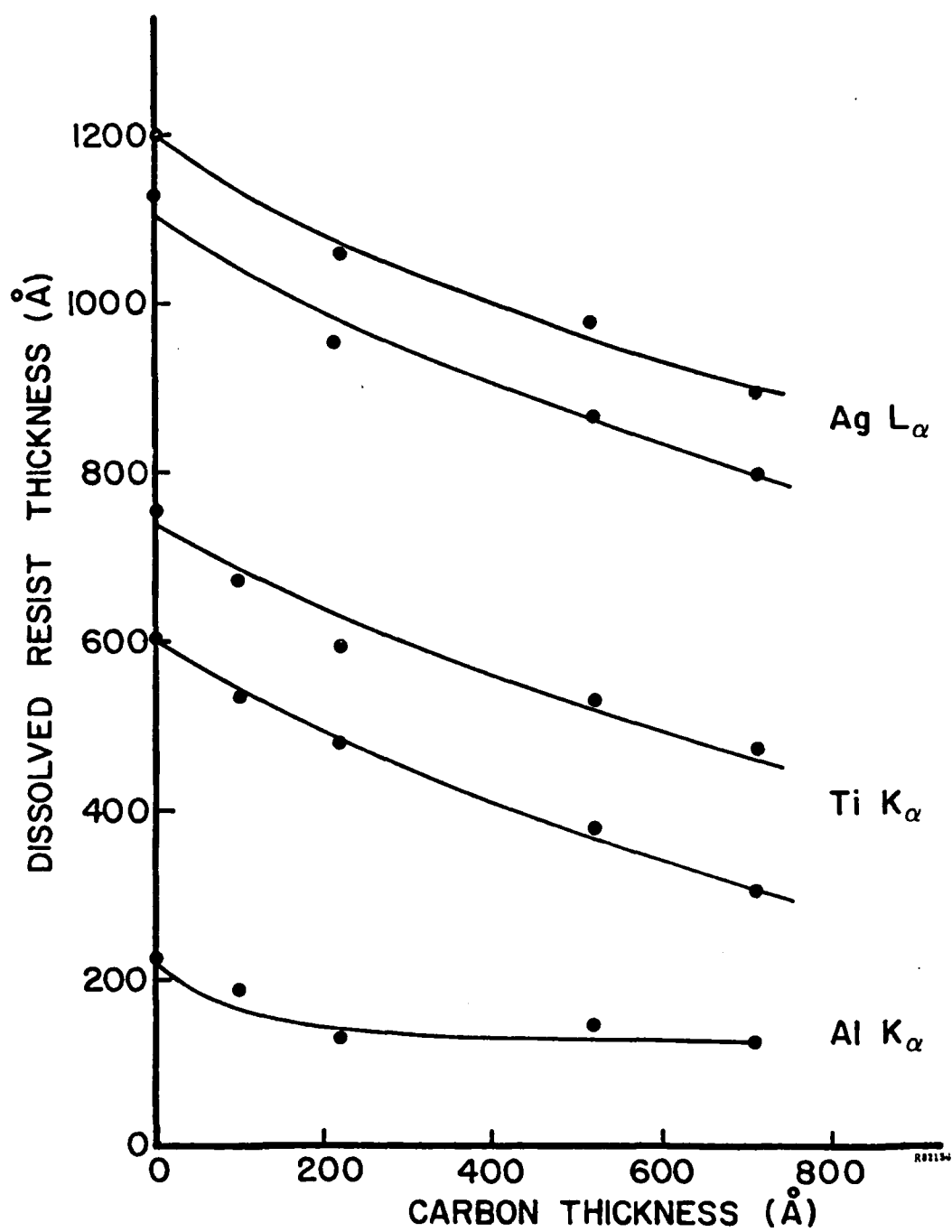


FIGURE 18. DOSE PROFILES IN PBS RESIST USING Au/C MASK
(Data plotted from Ellipsometer Measurements
such as Tabulated in Table 2.)

REFERENCES

1. Green, M. and Cosslett, V. E., "Measurement of K, L and M Shell X-ray Production Efficiencies," Brit. J. Appl. Phys. 2, 91), 425 (1968).
2. Sullivan, Paul A., "X-ray Lithography System Complete with interdigital Transducer System," Report No. AFCRL-TR-75-0573, Hughes Research Laboratories, 1975.
3. L. F. Thompson and M. J. Bowden, J. Elect. Chem. Soc. 120, 1722 (1973).
4. P. D. Blais, "X-ray Resist Technology" Kodak Microelectronics Seminar Proc., Interface p80, Kodak Report No. G-130 p. 79.
5. P.D. Blais, Westinghouse Research Center, Pittsburg, PA, private communication.



MISSION of *Rome Air Development Center*

RADC plans and executes research, development, test and selected acquisition programs in support of Command, Control Communications and Intelligence (C³I) activities. Technical and engineering support within areas of technical competence is provided to ESD Program Offices (POs) and other ESD elements. The principal technical mission areas are communications, electromagnetic guidance and control, surveillance of ground and aerospace objects, intelligence data collection and handling, information system technology, ionospheric propagation, solid state sciences, microwave physics and electronic reliability, maintainability and compatibility.

END

FILMED

12-83

DATIC